Accepted Manuscript

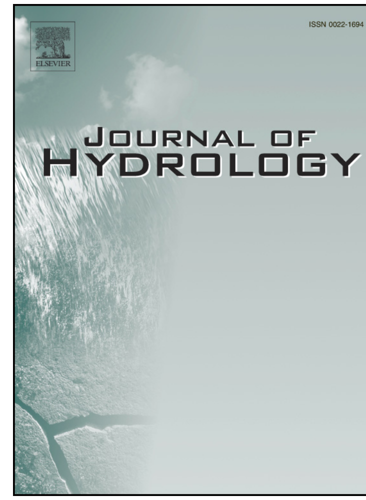

Detection and attribution of trends in magnitude, frequency and timing of floods in Spain

Luis Mediero, David Santillán, Luis Garrote, Alfredo Granados

PII: S0022-1694(14)00500-9
DOI: http://dx.doi.org/10.1016/j.jhydrol.2014.06.040
Reference: HYDROL 19714

To appear in: *Journal of Hydrology*

Received Date: 26 November 2013
Revised Date: 17 June 2014
Accepted Date: 23 June 2014

Detection and attribution of trends in magnitude, frequency and timing of floods in Spain

Luis Mediero[1], David Santillán, Luis Garrote and Alfredo Granados

Technical University of Madrid, Department of Civil Engineering: Hydraulic and Energy, 28040, Madrid, Spain

Abstract

An analysis to detect trends in magnitude, frequency and timing of floods was conducted in Spain through nine flood indicators. A data set of gauging stations where the effect of dam regulation on flow series is negligible was obtained. Annual maximum and peaks-over-threshold series were extracted in three periods: 1942-2009, 1949-2009 and 1959-2009. A pre-whitening procedure was applied to remove serial correlation and the Mann-Kendall test selected to detect trends. A general decreasing trend in magnitude and frequency of floods was detected in the three periods, with more notable evidence in 1959-2009. An increasing trend in the timing (i.e. towards later floods) was also found in the northwest of Spain. In addition, a study to relate detected flood trends to a set of potential drivers was also conducted. Most such trends in flood series could be explained by corresponding and increasing trends in evapotranspiration that increase water losses in soils and decrease soil moisture content before the occurrence of floods.

Keywords: Flood trends; Maximum annual series; Peaks-over-threshold series; Non-stationarity; Spain

[1] Corresponding author. Tel.: +34 91 336 5261; fax: +34 91 336 6764
E-mail address: luis.mediero@upm.es

1. Introduction

Reliable flood estimates for a given exceedance probability are crucial for hydrological risk analysis, as extreme flood events may lead to catastrophic effects on the environment, individuals and society. Unfortunately, extreme flood events have become more frequent and harmful in Europe for the last 25 years regarding the duration and extension of affected areas (Kundzewicz et al., 2013). In addition, their economic impact also increased for the period 1971 to 2008 (Barredo et al., 2012).

Traditional flood frequency analyses usually assume homogeneity, independence and stationarity in observed series (Rao and Hamed, 2000). However, stationarity is under doubt because means and extremes of precipitation and river streamflows could be changing in time, as a consequence of climate change (Milly et al., 2008) or any other driver. Consequently, non-stationarity assumptions question the results of traditional flood frequency analyses, which might lead to catastrophic failures in the case of underestimation and waste of economic resources in that of overestimation (Khaliq et al., 2006).

Several factors can cause changes in flood time series, such as climate change, wildfires, land-use changes, anthropogenic actions, relocation of gauging stations or volcanic eruptions (Yue et al., 2012). The latter entails a factor that can either change the soil properties in the catchment or modify the drainage network and its hydraulic properties by the deposition of erupted sediments. Climate drivers can be distinguished from anthropogenic-induced changes when the study focuses on pristine basins with reduced human interventions (Svensson et al., 2006).

Several flood trend analyses have been carried out recently in Europe. Wilson et al. (2010) analysed trends in annual and seasonal flows in near-natural catchments in

Denmark, Finland, Iceland, Norway and Sweden, detecting both a general increasing trend in streamflow magnitude and a trend in the timing of floods in the Nordic countries (except Iceland), given that they tend to arrive earlier in spring. Petrow and Merz (2009) found significant upward trends in flood magnitude and frequency in the south, west and centre of Germany. Significant upward trends in flood magnitude were also found in some Swiss alpine catchments (Castellarin and Pistocchi, 2012). Blöschl et al. (2012) found a general increasing trend in flood magnitude in Austria, especially in catchments of fewer than 500 km^2. While Giuntoli et al. (2012) found generalised upward trends in magnitude in the northwest of France, they identified downward trends in the southwest and mixed patterns in the centre. Hannaford and Buys (2012) found heterogeneous patterns in the United Kingdom, with an overall increasing trend in autumn and winter flows, a decreasing trend in spring flows in lowland England and a mixed pattern in summer. In addition, a general upward trend in flood magnitude was detected in Wales by Macdonald et al. (2010) and in Ireland by Murphy et al. (2013). Some Pan-European studies have also focused on monthly, seasonal and annual streamflows, as well as various streamflow indices (Stahl et al., 2010; Stahl et al., 2012; Hannaford et al., 2013).

Regarding trend studies beyond Europe, Ishak et al. (2013) found more generalised decreasing trends in annual maximum flood series in Australia, at both local and regional scales. Burn et al. (2010) found decreasing trends in both magnitude and timing of annual and spring maximum flows in Canada. Hodgkins and Dudley (2006) detected significant earlier flows in eastern North America. In addition, some studies have provided a global dimension, with Kundzewicz et al. (2005) analysing trends in streamflow series from catchments located around the world by using a subset of data extracted from the Global Runoff Data Centre (GRDC).

Most trend studies in Spain are focused on annual, seasonal and monthly flows. Lorenzo-Lacruz et al. (2012), for example, found downward trends in monthly streamflows in winter and spring across the Iberian Peninsula, particularly in the centre and south in the period 1945-2005. These results are in line with the Morán-Tejeda et al. (2011) study that detected a generalised negative trend in winter and spring monthly streamflows in the Douro catchment in the period 1961-2006. Both studies attributed part of these downward trends to the effects of dam regulation and water management strategies on flood regimes. However, a set of near-natural catchments in Spain was considered by Martínez-Fernández et al. (2013), who found negative trends in annual and seasonal streamflows in spring and winter in most catchments in the period 1966-2005. Finally, Stahl et al. (2010) also detected a general decreasing trend in both annual and monthly streamflows in Spain in the periods 1952-2004 and 1962-2004 that could, arguably, be caused by an increasingly positive trend in the North Atlantic Oscillation Index.

Certain local studies have analysed trends in floods in Spain. López-Moreno et al. (2006) analysed daily discharge series in the central Pyrenees on the Spain side for the period 1959-1995, finding a decreasing tendency in the frequency and magnitude of flood events. Since an overall downward trend in rainfall observations was not identified, flood trends were related to land use changes. A general decreasing trend in floods was also found in the Douro catchment in 1961-2005 by Morán-Tejeda et al. (2012).

Some trend studies in precipitation have been also carried out in Spain. López-Moreno et al. (2009) analysed time series of cumulative rainfall in five days in the Ebro catchment in the period 1955-2006 with downward trends being found in the central area of the catchment. These results are consistent with the conclusions reached by

Valencia et al. (2012) for the period 1957-2002. Turco and Llasat (2011) analysed the extreme rainfall variability in Catalonia for the period 1951-2003 with no consistent regional trend patterns identified. Acero et al. (2012) carried out a trend study on cumulative rainfall from one to seven days in the Iberian Peninsula for the period 1958-2004, with varying results offered depending on the season. In winter, a general negative trend was detected, except for positive trends at the south-eastern Mediterranean coast. In spring, a general negative trend was also detected, except for some positive trends in the northeast. However, whereas positive trends were detected in the west of the peninsula in autumn, negative trends were highlighted in the east.

In addition, temporal trends can be studied in reconstructed flood series by extending systematic records across several centuries by using historical and palaeoflood information (Llasat and Barriendos, 2001; Llasat et al., 2003). A thorough review and compilation of historical floods in Europe can be found in Brazdil et al. (2012). In Spain, this approach has been applied to the Rivers Ter, Llobregat and Segre in Catalonia, where no homogeneous behaviour has been observed for extraordinary floods from the 14th century to the present (Barriendos et al., 2003).

Summarising, most trend studies in flow series previously developed in Spain were focused on annual and monthly flows, which are essential for management of water resources and droughts. However, flood frequency analyses should account for a shorter temporal resolution, either instantaneous or mean daily, to characterise better peak flows. Some of the aforementioned trend analyses recently conducted in Spain have focussed on daily flows. Nevertheless, they focus only on some local regions of Spain, such as the Ebro and Douro catchments.

In this paper, a flood trend analysis is carried out at a national scale in Spain with the aim of filling an existing research gap. The analysis focuses on tendencies in magnitude, frequency and timing of floods through using observed daily flow series. A set of catchments where effects of dam regulation on floods can be neglected is selected from the results of a thorough screening of the Spanish flood data conducted previously by Jiménez-Álvarez et al. (2012). This data set also complements previous research studies regarding long and unaffected flow time series to be used in flood studies in Spain. Nine flood indicators obtained from annual maximum, seasonal maximum and peaks-over-threshold (POT) series are used. Three periods are considered in accounting for larger temporal extension at the expense of poorer spatial coverage and vice versa. A study to link detected significant trends in flood series to different drivers is undertaken through a set of indices based on both daily precipitation and temperature series . The partial Mann-Kendall test is used to assess the influence of each climate variable on flood trends.

The paper is organised as follows: Section 2 introduces the methodology; Section 3 summarises the case study and data used; Section 4 presents the results; Section 5 is devoted to the discussion of the results presented in the previous section; finally, conclusions are included in Section 6.

2. Methodology

In this section, the method used to detect trends in flood series based on the Mann-Kendall (MK) test is presented. Second, the influence of both the selected period of time and the spatial correlation among sites on detecting significant trends is analysed. Then, a summary of the hydrological variables used is provided. Finally, the methodology to link flood trends to a set of climatic variables used as surrogates of flood drivers is offered.

2.1. Detection of monotonic trends

Temporal trends can be classified into step-changes and monotonic trends. The former assumes that the observed data show an abrupt change at a given time, while the latter involves a gradual change in time (Yue et al., 2012).

Temporal trends are customarily detected by statistical tests, which can be also classified into parametric and non-parametric or distribution-free tests. The former requires independent and normally distributed data, while the latter assumes that data are independent and identically distributed. Non-parametric tests are particularly suitable for flood series, as hydrological data are usually non-normal distributed and serially correlated (Kundzewicz and Robson, 2004). Moreover, they are more robust to outliers and do not require any assumption related to the distribution (Hamed and Rao, 1998).

Two common non-parametric tests are used for monotonic trend detection: the MK and Spearman's rho. Both have been recommended by the World Meteorological Organization (Chebada et al., 2013) and have the same power (Yue et al., 2002). Both consider the null hypothesis, H_0, that there is no trend while the alternative hypothesis, H_1, assumes that there is a trend.

In this paper, the MK test was selected. The MK test statistic, S, is defined by Eq. 1.

$$S = \sum_{i=1}^{n-1} \sum_{j=i+1}^{n} sgn(X_j - X_i) \tag{1}$$

$$sgn(\theta) = \begin{cases} 1 \text{ for } \theta > 0 \\ 0 \text{ for } \theta = 0 \\ -1 \text{ for } \theta < 0 \end{cases} \quad (2)$$

where X_i and X_j are the sequential data values and n is the record-length. Significant trends were detected for p-values with a significance level of less than 5%. The magnitude of a significant trend was estimated by Sen's slope (Sen, 1968) (Eq. 3).

$$\beta = median\left(\frac{X_j - X_i}{j - i}\right) \forall\, i < j \quad (3)$$

where β is the estimate of the slope of the trend in m^3/s. As β depends on the magnitude of floods and, subsequently, on the catchment area, β values are not comparable among sites. In this way, β has been standardised by the mean of the flood series.

Robust results of the MK test are achieved when time series do not show serial correlation. Should positive serial correlation exist, the probability of detecting a significant trend increases (Kulkarni and von Storch, 1995). Pre-whitening (PW) was developed to remove the lag-1 serial correlation of a time series before applying the MK test (von Storch, 1995). However, PW can either reduce or enlarge temporal trends. Therefore, the trend-free pre-whitening (TFPW) procedure was developed by Yue and Wang (2002). In other studies, some modifications of the MK test have been also proposed. For example, Hamed and Rao (1998) developed a theoretical relationship for calculating the variance of the MK test when a time series shows serial autocorrelation. Hamed (2009) improved the calculation of the variance of the MK test through a beta distribution. Onoz and Bayazit (2012) determined the optimal block length that minimises errors of the block bootstrapping MK test (BBMK) and concluded that the power of the BBMK test is comparable with the power of the modified MK tests based on variance correction. In addition, the TFPW test showed a higher power than the

BMMK. In this paper, the original MK test is preferred and autocorrelation is removed from the time series through the TFPW procedure.

TFPW consists of several steps. First, the magnitude of the trend (β) in the time series of a random variable $X_1, X_2, \dots X_T$ is estimated by Sen's slope (Eq. 3). Then, the trend is removed and a new time series, $Y_1, Y_2, \dots Y_T$ obtained by Eq. 4. Next, the autocorrelation for one lag time step, ρ_1, is estimated and removed from the time series, obtaining another series, $Y_1', Y_2', \dots, Y_T'$ (Eq. 5). The removed trend, β, is returned again to the time series $Y_1'', Y_2'', \dots, Y_T''$ (Eq. 6), where the MK test is applied.

$$Y_t = X_t - \beta t \tag{4}$$

$$Y_t{}' = Y_t - \rho_1 Y_{t-1} \tag{5}$$

$$Y_t'' = Y_t{}' + \beta t \tag{6}$$

where t is the time.

2.2. Influence of data length on the MK results

The results of the MK test can depend strongly on the period of time considered. Merz et al. (2012b) showed that the validity of the results can be conditioned to the selection of the starting and ending years of the time series. Moreover, given either starting or ending years, this could lead to detecting significant trends, when this trend disappears over the long-term natural variability. Furthermore, moving the years slightly to the past or future can make the trend disappear in some cases.

A sensitivity analysis of the selected period of time on the MK results was conducted, accounting for the longest flow series. The MK test was repeatedly calculated, by using a moving window of varying length, to identify periods that lead to a misleading detection of trends.

2.3. Influence of spatial correlation on the MK results

Spatial correlation among sites can lead to a larger probability of detecting significant trends. Such detected trends at several sites can be transformed into an insignificant trend at the regional scale when accounting for spatial correlation. Therefore, a field significance test should be applied to detect significant trends in a region where cross-correlation among sites exists. In this paper, the bootstrap test proposed by Yue et al. (2003) has been applied as follows:

1. A bootstrap is applied to the year series of the period of interest, resampling them randomly with replacement. A set of N synthetic series of years is obtained with the same length as the original series, though with different year orders.
2. Observations at each year and each site of the original series are rearranged according to the new synthetic series obtained in the previous step. Spatial correlation among sites is preserved, while the temporal order is randomised. N synthetic regions of m sites are obtained. Therefore, Nxm synthetic series of floods are obtained.
3. The MK test and its corresponding p-value are obtained for each synthetic series of floods. The number of sites with a significant upward trend (N^{*}_{up}) and the number of sites with a significant downward trend (N^{*}_{down}) are counted in each synthetic region. A series of N^{*}_{up} and N^{*}_{down} of length N are obtained.
4. The bootstrap empirical cumulative distribution (ECD) of the series of N^{*}_{up} and N^{*}_{down} obtained in the previous step are calculated. The probability (p_{obs}) of the observed number of significant upward trends (N_{up}) and downward trends (N_{down}) in the real region are calculated from the ECD of N^{*}_{up} and N^{*}_{down} by Eq. 7-8. Their corresponding p-value (p_F) is given by Eq. 9. If p_F is smaller than the significance level, the trend is considered as field-significant.

$$p_{obs}^{up} = P(N_{up} \leq N_{up}^{*}) \tag{7}$$

$$p_{obs}^{down} = P(N_{down} \leq N_{down}^{*}) \tag{8}$$

$$p_F = \begin{cases} p_{obs} & if\ p_{obs} \leq 0.5 \\ 1 - p_{obs} & if\ p_{obs} > 0.5 \end{cases} \tag{9}$$

2.4. Hydrological variables

The hydrological variables used for trend detection are listed in Table 1. Annual maximum flood series (AMF) were obtained from the daily flow series, as the maximum value in a hydrological year from October to September. However, several large floods are usually overlooked in AMF series, as only the largest flood in a hydrological year is identified. POT series overcome this drawback by accounting for all the floods that exceed a given threshold regardless of the time they have occurred. In such a way, unimportant small floods identified in the AMF series as the largest in dry years are ignored. In addition, POT series supply more information about floods, such as their magnitude, timing, waiting time between two successive peaks and clustering in time. POT series were obtained from the daily flow series by using an independence criteria between two successive peaks given by Eq. 10 and 11 (Lang et al., 1999). Another improvement of POT series on the AMF series entails consideration of a larger number of floods. As it is commonly assumed that a POT series improves an AMF series in the case of a minimum of two or three events per year on average, a threshold that leads to three events per year on average (POT3) was used.

$$\theta > 5 + log(0.3861\ A) \tag{10}$$

$$Q_{min} < \frac{3}{4} min(Q_1,\ Q_2) \tag{11}$$

where θ is the lag time between two successive peaks, A is the catchment area in km^2 and Q_{min} is the minimum discharge between two successive peaks Q_1 and Q_2.

The mean day of flood (MDF) was used to characterise the timing of the POT series. It is computed by a directional statistic that characterises dates of flood occurrence as vectors (Macdonald et al., 2010). The day of occurrence of the i POT event in the j hydrological year, DF_{ij}, is transformed into an angular value, θ_{ij} (Eq. 12). Then, the directional mean of year j, $\overline{\theta_J}$, or MDF_j is computed by Eq. 13.

$$\theta_{ij} = DF_{ij}\frac{2\pi}{LY_j} \tag{12}$$

$$\overline{\theta_J} = \tan^{-1}\frac{\bar{x}}{\bar{y}} \;\; ; \;\; MDF_j = \bar{\theta}_j\frac{LY_j}{2\pi} \tag{13}$$

$$\overline{x_J} = \frac{1}{I_j}\sum_{i=1}^{I_j}\cos\theta_{ij} \;\; ; \;\; \overline{y_J} = \frac{1}{I_j}\sum_{i=1}^{I_j}\sin\theta_{ij} \tag{14}$$

where LY_j is the number of days in the j hydrological year and I_j is the number of events in the j hydrological year.

2.5. Link to climatic variables

Different flood drivers could, it might be argued, have influence on trends (Merz et al., 2012a): first, meteorological forcing drivers in the atmosphere, such as trends on precipitation series; second, climatic drivers that have influence on the antecedent moisture content (AMC) in the catchment, such as temperature, annual precipitation and evapotranspiration, among others; third, rainfall-runoff generation and concentration processes in catchments, such as changes in either runoff coefficients or initial abstractions in the case of surface flows, and infiltration rates and water storage capacities, in the case of subsurface flows; and fourth, flood propagation processes in rivers that depend on river morphology and extension of flood prone areas, among others.

In this study, detected trends in flood series were related to meteorological, climatic and rainfall-runoff generation and concentration drivers. A data-based approach was used, focusing on precipitation and temperature time series, from which a set of variables were inferred as surrogates of flood drivers. It should be noted that the influence of drivers on each flood event is beyond the scope of the paper, as the focus is on trends in time series.

2.5.1. Climatic variables

First, the possible influence of meteorological forcing drivers was tested by analysing trends in annual maximum cumulative precipitation on one, three and five days (AMP1, AMP3 and AMP5). Floods in small catchments can be driven by rainfall events of shorter durations. However, sub-daily precipitation time series are not freely available in Spain. Second, the magnitude of floods also depends on the AMC in the catchment before the occurrence of a flood event. The larger is the AMC, the larger is the flood peak for the same rainfall event. Furthermore, no trend in precipitation extremes could lead to a decreasing trend in floods, when the climate tends to be dryer and, consequently, smaller AMCs are more likely to appear before flood events. The AMC in a catchment depends on both the antecedent evapotranspiration that decreases the soil water storage and the antecedent precipitation that increases the soil water storage. Three variables were used to explain the probability of initial moisture content before a flood event: first, annual cumulative precipitation (*AP*); second, annual cumulative evapotranspiration (*ET*); and third, the antecedent precipitation index (*API*). The first and second give information about yearly gains and losses of water storage in the catchment, while the third is used to approximate the AMC when soil moisture measurements are not readily available (Pui et al., 2011).

ET was obtained from temperature daily series through the Hargreaves equation (Eq. 15) (Hargreaves and Allen, 2003). This method was used as additional observed data, such as net radiation, wind speed and relative humidity, are not available in the catchments of study (Shuttleworth, 1993).

$$ET = 0.0023\, R_a\, (TC + 17.8)\, TR^{0.5} \tag{15}$$

where R_a is the water equivalent of extraterrestrial radiation (mm), *TC* is the temperature in degrees Celsius and *TR* is the daily temperature range in degrees Celsius computed as the mean daily maximum temperature minus the mean daily minimum temperature.

API assumes that AMC only depends on rainfall. AMC depends largely on rainfall that occurs closer in time to the flood event, though the influence of previous rainfall decreases. Consequently, *API* before a flood event is calculated by Eq. 16 (Kohler and Linsley, 1951).

$$API_i = kP_{i-1} + k^2P_{i-2} + \ldots + k^qP_{i-q} \tag{16}$$

where i is the day when the flood event occurs, P_i is the daily precipitation on day i (mm), k is a recession factor that depends on the catchment characteristics and q is the maximum previous time for which the antecedent rainfall influences AMC (days). As water soil content measurements are not available in the catchments studied, a value of 0.90 has been taken for k and a period of 14 days adopted for q (Heggen, 2001).

Finally, changes in rainfall-runoff processes at the catchment scale can also drive flood trends. They can be caused by the following: first, land use changes, such as deforestation or forestation, urbanisation, wildfires and agricultural use changes that lead to changes in both surface runoff and infiltration rates; and second, changes in water tables caused by either overexploitation or recharge of aquifers that lead to changes in subsurface runoff flows and water storage capacity in soils. Moreover, these changes in rainfall-runoff processes also lead to changes in the catchment water balance in addition to both *ET* and precipitation. Consequently, the ratio of annual runoff at the gauging station to precipitation in the catchment (*AR/AP*) was used as a simplified surrogate to detect trends in the catchment water balance that could lead to flood changes. However, *AR/AP* cannot differentiate the influence of *ET* on the water balance from that of rainfall-runoff processes. Therefore, the results of *AR/AP* should be compared to those of *ET* to find whether *ET* or rainfall-runoff processes is the main driver of change in floods.

2.5.2. Statistical analyses

Trends in these climatic variable series in hydrological years were tested. However, a significant trend in any of these variables could not lead necessarily to a significant trend in the flood series. Consequently, the correlation between these variables and flood time series was examined. Climatic variable series at the gauging stations were obtained from averaged daily values of the precipitation and temperature time series in the catchment, accounting for the set of grid cells overlapping each catchment.

In addition, the partial Mann-Kendall (PMK) test proposed by Libiseller and Grimvall (2002) was used to detect trends in the dependent variable (flow series) after removing the effect of a covariate (climatic variable series) (Eq. 17). PMK analyses if the detected trend in the dependant variable is significant after accounting for the correlation with a covariate variable. If the p-value of the PMK statistic is larger than the significance level of 5%, the detected trend is removed and can be linked to the covariate variable.

$$PMK = \frac{S_y - \rho S_x}{\sqrt{\frac{(1-\rho^2)n(n-1)(2n+5)}{18}}} \tag{17}$$

where S_y is the MK statistic of the dependent variable, S_y is the MK statistic of the covariate variable and ρ is the correlation between S_x and S_y.

3. Case study and data

Spanish catchments are managed by 16 river basin authorities (RBAs) (Figure 1), mainly based on hydrologic and geographical boundaries. Nine of them are trans-regional and are run by the Ministry of the Environment. The other seven are regional and depend on corresponding self-governing regions. Daily discharge series are provided freely by both the Centre for Hydrographic Studies of CEDEX and the Integrated System of Water Information. However, data from gauging stations located in some of the regional RBAs are not freely available. Consequently, spatial coverage of this study shows some blank areas. In addition, while most gauging stations are clustered in the north part of Spain, the southern part shows a less dense coverage. This is caused by either a major dam regulation of catchments or a less dense hydrometric system with shorter records. Regarding temporal coverage, the longest flow series have records from 1912 to 2009. Unfortunately, the records have a gap in the period 1936-1942, because of a lack of data during and some time after the Spanish Civil War.

A screening of the flow data obtained for Spain was conducted previously by Jiménez-Álvarez et al. (2012) to develop a national map of flood discharges in Spain. In this study, gauging stations located in catchments where flood control processes in reservoirs could change natural flood regimes were removed. In addition, stations with possible changes in either location or rating curves, frequent gaps in records and discordant magnitude or timing of floods in comparison with neighbouring catchments were also discarded. From this data set, stations with a continuous record in three common temporal periods of at least 40 years up to the present were selected. The longest period extends from 1942 to 2009, with only 10 gauging stations accounting for the longest series after the gap 1936-1942. Another two shorter periods were used, from 1949 to 2009 with 42 gauging stations and 1959 to 2009 with 61 gauging sites (Table 2).

The spatial distribution of the selected gauging sites is depicted in Figure 1. While catchment areas range between 28 km^2 and 2,413 km^2, the average is 362 km^2. No sites with a sufficiently long temporal extension were found in the Segura catchment. A reduced set of gauging stations was obtained in the Tagus catchment as most of the tributaries are regulated by large dams. Most gauging stations in the Guadiana and Guadalquivir catchments had short and discontinuous records. Flow data are not freely available for the Galician Coast, Mediterranean Andalusian and Basque Country RBA.

Precipitation and temperature daily series were obtained from the freely available gridded dataset Spain02, which was developed by applying the Kriging method to observations recorded at 2,756 rain gauging stations (Herrera et al., 2012). The dataset is based on a gridded map with resolution of 0.2º. Daily time series from January 1949 to March 2008 are supplied in each cell, though it should be noted that continuous data series are only available for the hydrological years 1949-2006.

4. Results

First, the results of flood trends in AMF and AMFD are presented. Second, trends in seasonal maximum floods are analysed. Third, the results of trends in POT3 series regarding magnitude, frequency and timing are described. Then, the influence of the selected record length and the spatial correlation on the results of the MK test is analysed. Finally, the link of flood trends to climatic variables is presented.

4.1. Trends in AMF magnitude and timing

A general downward trend in AMF series was found for the three periods. For the period 1942-2009 (Fig. 2a), decreasing trends were found in five of 10 sites, clustered in the centre of Spain: in the south-western Douro and heads of the Tagus and Júcar catchments. For the period 1949-2009 (Fig. 2b), generalised downward trends extend to the northern Ebro catchment. However, two increasing trends were detected in both the Cantabrian RBA and the head of the Douro catchment. For the period 1959-2009 (Fig. 2c), the general downward trend extends to the north-western, southern and north-eastern parts of Spain. Only a gauging station in the River Sella shows a clear increasing trend. It can also be seen that slopes of trends become larger as the starting year moves forward.

Regarding the timing of AMF, tendencies in the AMFD series were investigated. Only one gauging station in the Ebro catchment showed a significant decreasing trend for the period 1942-2009 (Fig. 2d). This trend disappears when the starting year of the series moves forward. Only two significant increasing trends were found for the period 1949-2009, at two sites at the heads of the Ebro and Júcar catchments (Fig. 2e). In addition, a downward tendency was detected in the eastern Pyrenees of the Catalonian RBA. Nevertheless, a more general and increasing tendency in the northeast of Spain was detected for the period 1959-2009 (Fig. 2f). Consequently, floods tend to occur later in some sites of the Douro, Ebro and Júcar catchments, as well as the Catalonian RBA in the period 1959-2009.

In summary, a general decreasing trend in AMF series was found in most of the stations considered, with this becoming more evident and stronger for the period 1959-2009 than 1942-2009. In addition, the day of occurrence of AMF tends to occur later in the north-eastern part of Spain for the period 1959-2009.

4.2. Trends in seasonal floods

Trends in the magnitude of floods in each season were analysed (Fig. 3). In autumn, only two decreasing tendencies were detected in the Júcar and Ebro catchments in the period 1942-2009 (Fig. 3a). However, a clearer pattern of decreasing trends was found in the northeast of Spain (Ebro and Júcar catchments) for the period 1949-2009 (Fig. 3b). This pattern becomes more evident for the period 1959-2009 (Fig. 3c). Decreasing trends extend to the head of the Guadiana catchment, as well as to the Catalonian RBA. No evidence of trends was found either in the Douro and Tagus catchments, or in the Minho-Sil RBA. The spatial pattern of decreasing trends in autumn floods becomes more evident as the starting year moves forward. Furthermore, slopes of trends become larger as the starting year moves forward.

In winter, downward tendencies were found both in the southern Douro and the heads of Tagus and Júcar catchments for the period 1942-2009 (Fig. 3d). This pattern becomes clearer for the period 1949-2009 with two clusters: first, eastern Minho-Sil RBA and north-western Douro catchment; and second, Ebro, Júcar and the head of the Tagus catchment, as well as south-eastern Catalonian RBA (Fig. 3e). The decreasing pattern of winter floods becomes general in almost all sites considered for the period 1959-2009 (Fig. 3f). In addition, slopes of trends become larger as the starting year moves forward. However, some local increasing trends were detected in both the Guadiana catchment and the Cantabrian RBA.

In spring, a scattered pattern is identified for the period 1942-2009 (Fig. 3g). More decreasing trends were found for the period 1949-2009, mainly in the eastern Minho-Sil RBA, north-western Douro, the head of the Júcar catchment, northern Ebro and eastern Catalonian RBA (Fig. 3h). For the period 1959-2009, some more evident clusters of downward trends were found in: first, south-eastern Cantabrian RBA, eastern Minho-Sil RBA and north-western Douro catchment; second, southern Ebro and the head of the Júcar catchment; and third, northern Ebro catchment and eastern Catalonian RBA (Fig. 3i). No evidence of trends was found in the south-western part of Spain. In this case, slopes of trends also become larger as the starting year moves forward.

In summer (Fig. 3j-l), a clear pattern of decreasing trends was found in almost all stations for the three periods (mainly in the eastern Minho-Sil RBA, Douro and Ebro catchments, Catalonian RBA, head of the Tagus and Júcar catchments). The pattern becomes more clear and stronger as the starting year moves forward. No evidence of trends was found in the Cantabrian RBA.

In summary, general decreasing trends were found in all seasons for the three periods, except for some increasing trends detected in the central northern part of Spain in winter. Specifically, autumn floods showed a decreasing trend in the eastern part of Spain, while a general decreasing pattern was found in almost all sites considered in the study in winter. However, in spring the pattern was more clustered in: first, south-eastern Cantabrian RBA, eastern Minho-Sil RBA and north-western Douro catchment; second, southern Ebro and the head of the Júcar catchment; and third, northern Ebro catchment and eastern Catalonian RBA. Finally, a general decreasing pattern was also found in almost all sites considered in the study in summer.

4.3. Trends in POT3 magnitude, frequency and timing

An analysis of trends in magnitude, annual frequency and timing of floods was carried out based on the POT3 series. The results are presented in Figure 4. Regarding the magnitude of floods, no evidence of general trends was found for the period 1942-2009 (Figure 4a), as only one increasing trend was detected in the Douro catchment and two decreasing trends in the Ebro and Júcar catchments. More evident decreasing trends were found for the period 1949-2009 in the northern part of the Ebro catchment and in central Spain, while increasing trends were found in the Minho-Sil and northern Catalonian RBA (Figure 4b). Decreasing trends become more general in the period 1959-2009, extending to most Ebro catchment, eastern Minho-Sil RBA and north-western Douro catchment (Figure 4c). An increasing trend was found in the Catalonian RBA. This pattern confirms the decreasing trend pattern found in AMF series, although POT3 shows less and smaller decreasing trends.

A general decreasing pattern was detected in annual frequency of flood events for the three periods (Figure 4d-f). The pattern becomes more evident as the starting year moves forward and more gauging stations are included in the analysis. However, an increasing trend in frequency was found at one site in the central-northern part of Spain. This site also showed an increasing trend in AMF.

Trends in the timing of the POT3 series can be found in Figure 4g-i. No trend patterns were found for the periods 1942-2009 and 1949-2009. However, an increasing trend pattern was found in north-eastern part of Spain, following the results of the AMF series.

In summary, decreasing trends in POT3 magnitude were found in eastern Minho-Sil RBA, north-western Douro, Ebro and the heads of Tagus and Júcar catchments, confirming the decreasing trend pattern found in AMF series. A general decreasing pattern was also detected in annual frequency of POT3 series. Finally, an increasing trend pattern was found in north-eastern part of Spain for the period 1959-2009, also confirming the results found in AMF series. It becomes seems that floods tend to occur later in this part of Spain.

4.4. Influence of data length on the MK results

Significant trends in AMF and magnitude of POT3 series were examined by use of the MK test, taking a varying length moving window to analyse the dependence of results on the period considered.

The results for the 10 longest AMF series are depicted in Figure 5. Trends are not highly conditioned on the period of time selected, as the significance, positive or negative sign and magnitude of trends do not show large changes. However, some stations show periods with stronger tendencies, such as the D2, T2, J2 and E18 gauging stations that show a similar pattern. The series starting in the period 1950-1960 and ending in the period 1990-2000 lead to stronger decreasing trends. The D2 gauging station shows stronger decreasing trends when the starting year is between 1950 and 1960 and the ending year is between 1985 and 2000. A flood-rich period can be observed in the period 1950-1965, when most floods are larger than the series mean, while a flood-poor period in 1970-2000, when most floods are below the mean (Fig. 6a). The T2 gauging station shows larger decreasing trends when starting in the period 1955-1970 and ending in 1990-2010. A flood-rich period can be observed in 1955-1970, while a flood-poor period in 1990-2010 (Fig. 6b). In the case of E18, stronger decreasing trends are found in series starting in 1950-1965, corresponding to a flood-rich period, and ending in 1990-2005, also corresponding to a flood-poor period.

The results for the POT series can be found in Figure 7. Similar patterns to the AMF series were identified for gauging stations D2, T2, J5 and E18. Temporal patterns of AMF series found in gauging stations D3and J2 disappear in the POT series. Flood-rich and flood-poor periods in D2, T2 and E18 AMF series are confirmed by the annual flood occurrences of POT series (Fig. 8)

Conditional results of tendencies on given starting and ending years can be caused by flood-rich and flood-poor periods. A flood-rich period in 1950-1970 seems to occur in some regions of Spain. Consequently, general decreasing trends found for the period 1959-2009 in both AMF and POT3 series could be conditioned on this flood-rich period at the beginning of the series.

4.5. Influence of spatial correlation on the MK results

A field significance test was conducted to determine the effect of cross-correlation between pairs of sites on trend results. The bootstrap method described in Section 2.3 was applied to the whole set of gauging stations, as well as to the RBAs with a greater number of gauging stations: the Douro, Ebro and Júcar. The analysis was conducted for the periods 1942-2009, 1949-2009 and 1959-2009. However, the test was only conducted for the case of all stations in the period 1942-2009. The results can be found in Tables 3 to 5.

Most of the decreasing trends were found to be field-significant. Regarding all the stations, decreasing trends were field-significant for AMF, AMFAu, AMFWi, AMFSp, AMFSu and POT3F for the three periods. Decreasing trends in POT3M were field-significant only in the period 1959-2009. A field-significant trend in AMFD was found in 1942-2009, while no field-significant trends were detected in POT3MDF for any period of time.

In the Douro catchment, decreasing field-significant trends were found in AMF, AMFWi, AMFSp, AMFSu and POT3F for both periods. An increasing field-significant trend was also found in the period 1949-2009.

In the Ebro and Júcar catchments, field-significant decreasing trends were detected for AMF, AMFAu, AMFWi, AMFSp, AMFSu and POT3F in both periods. In addition, some increasing trends in the timing of floods of AMF and POT3 series were also found to be field-significant in 1959-2009.

4.6. Link to climatic variables

A study to relate detected trends in AMF series to potential climatic drivers was carried out. For the sake of simplicity, this section does not account for trends in POT3, as POT series of both precipitation and evaporation series were not obtained.

Meteorological drivers were accounted for by the maximum annual precipitation observed at durations of one, three and five days (*AMP1*, *AMP3* and *AMP5*) (Fig. 9a-c). Influence of climatic drivers on AMC was accounted for by *AP* (Fig. 9d), *ET* and *API* (Fig. 10a-b). Changes in rainfall-runoff processes were accounted for by *AR/AP* (Fig. 10c). These variables are based on precipitation and temperature time series that are available for the period 1949-2006, as noted above in Section 3. Consequently, the period 1959-2006 was considered for linking flood trends to climatic variables. Flood trends were re-calculated for this period for the sake of consistency, as slight differences were found from the periods used for detection of trends in flood series.

Trends in AMF series were detected at 34 gauging stations in the period 1959-2006. A summary of the trends detected in both AMF and climatic variable series for these sites can be found in Table 6. The results of the PMK test that detects trends in AMF series after accounting for the correlation with each climatic variable can be found in Table 7 and Fig. 9-10.

A general decreasing trend in AMF was also detected in this period. However, C2 showed an increasing trend, which could be linked to an increasing trend in *API*. Nevertheless, the significance of this trend could not be removed by any climatic variable (Table 7). It should be noted that most of the decreasing trends were explained by increasing trends in *ET*, as detected trends in AMF were removed after accounting for this climatic variable (Table 7 and Fig. 10a). MS3, D3 and D4 trends were also explained by *AR/AP*. However, the decreasing trend detected in the northern part of the Douro catchment (D8) could not be explained by any climatic variable. In the Tagus, Guadiana and Guadalquivir catchments, the decreasing trends in T1 and GQ1 were also explained by *AMP3*, *AMP5* and *AR/AP*, while the trend in GD1 was explained only by *AR/AP*.

In the Júcar catchment, most of the decreasing trends were linked to trends in *ET*. However, the trend in J6 was also linked to *AMP5*, *API* and *AR/AP*, while that in J7 was explained only by *AR/AP*.

Most of the decreasing trends in the Ebro catchment were linked to increasing trends in *ET*. However, different regional patterns were found in the Ebro catchment. Trends detected in the north-western part were also linked to decreasing trends in *AMP* (E1, E16 and E17). No drivers of trend could be linked to decreasing trends found in some gauging stations of the central part of the Ebro catchment (E10, E22 and E25). Gauging stations in the north-eastern and southern parts were linked to changes in *AR/AP*.

Finally, both flood trends detected in the Catalonian RBA were linked to *AR/AP*. However, the trend in CT2 was also linked to *ET*, while the trend in CT4 was also linked to *AP*.

In summary, most trends in AMF series were linked to increasing trends in *ET* that rise water losses in the catchment soil and, consequently, AMC. In addition, some trends could be also explained by *AR/AP* pointing to possible changes in either land use or water tables.

5. Discussion

A generalised decreasing trend was found in most flood variables in the set of sites considered in the study for the three periods. The spatial significance of these trends was confirmed after conducting a field significance test.

Decreasing trends in AMF, AMFWi, AMFSp, AMFSu and POT3F were found to be field-significant for the three periods in both all stations and the three catchments considered (Tables 3 to 5). A larger number of decreasing trends were found in AMFSu than in the other seasons when considering all stations, as well as in the Douro and Ebro catchments. In the Júcar catchment, more decreasing trends were found in both AMFAu and AMFWi. However, less significant decreasing trends were found in POT3M series in all cases. In addition, some of them were found to be not field-significant.

Regarding the timing of floods, some positive trends were found in AMFD and POT3MDF, mainly in the Ebro and Júcar catchments for the period 1959-2009. This points to a delay in the arrival of floods in these catchments in this period of time.

In general, these results agree with the studies carried out previously in Spain. López-Moreno et al. (2009) found a clear decreasing trend in the frequency and magnitude of floods in the central Pyrenees of the Ebro catchment in the period 1959-1995, which is in accordance with the results shown in Table 5. Morán-Tejeda et al. (2012) found a decreasing trend in AMF, AMFWi, AMFSp and AMFSu series in the Douro catchment in the period 1961-2005. A lower proportion of significant decreasing trends was found in AMFAu. These results are in agreement with those obtained in the Douro catchment for the periods 1949-2009 and 1959-2009 shown in tables 4 and 5. At a different time scale, other studies point in the same direction. For example, Martínez-Fernández et al. (2013) found decreasing trends in annual and spring and winter monthly flows in the period 1966-2005. And Stahl et al. (2010) also found decreasing trends in annual and monthly flows in a set of sites in the mid-north part of Spain in the periods 1952-2004 and 1962-2004.

The significance of most trends in AMF was removed after accounting for the correlation with *ET*. Decreasing trends in flood series seem to be linked to increasing trends in *ET* in the last decades that lead to drier conditions before the occurrence of a flood event. This result is in accordance with other studies, such as Sousa et al. (2011), who found a trend towards drier conditions in the north-western part of the Iberian peninsula in the 20th century, Moratiel et al. (2010), who detected a general decreasing trend in the relative humidity in Spain in the period 1973-2002, and del Río et al. (2011), who identified a general significant increasing trend in annual temperature in Spain in the period 1961-2006. Consequently, increasing *ET* seems to be caused by both increasing trends in temperature and decreasing trends in relative humidity. In addition, decreasing trends in floods cannot be linked to decreasing trends in precipitation, as trends in AMF series were not usually removed by any of the variables based on precipitation (*AMP*, *AP* and *API*).

In addition, changes in rainfall-runoff processes in the catchment that could be related to changes in land use and aquifer water tables explain decreasing trends in flood series in some sites where the trends could not be explained by *ET*. This follows the findings of López-Moreno et al. (2006) in the Ebro catchment, where flood trends were linked to land use changes, as trends in precipitation were not found.

Summarising, decreasing trends in flood series seem to be driven by increasing trends in *ET* and changes in land use and water tables, rather than by trends in precipitation. Nevertheless, these findings should be confirmed by a further study based on simulation.

6. Conclusions

An analysis of trends in magnitude, frequency and timing of floods was conducted in 61 gauging stations in Spain through nine flood indicators in the periods 1942-2009, 1949-2009 and 1959-2009. A study to link these detected trends to a set of seven climatic variables was also conducted in the period 1959-2006.

A general decreasing trend in annual maximum series was found in Spain in the three periods, with more notable evidence in the period 1959-2009 than 1942-2009. Autumn floods showed a decreasing trend in eastern Spain, mainly in the Ebro and Júcar catchments. A general decreasing pattern was found in winter, spring and summer. Regarding the peaks-over-threshold series, decreasing trends in magnitude were found in the northwest of Spain in 1949-2009 and 1959-2009 (the Ebro and Júcar catchments). Furthermore, a general decreasing pattern in the frequency of flood events was found in the three periods, with floods tending to occur later in the Ebro and Júcar catchments over the period 1959-2009. However, these general decreasing trends could be conditioned on a flood-rich period observed in 1950-1970 in some parts of Spain, which would be placed at the beginning of the flood series.

Detected trends in flood series were linked to increasing trends in evapotranspiration that increase the loss of water in soils and reduce moisture content in the catchment before the occurrence of flood events. The variables based on precipitation could not explain most flood trends. Consequently, decreasing trends in flood series seems to be related to increasing temperatures and decreasing relative humidity in last decades.

Acknowledgements

The authors would like to thank Ataur Rahman and Jamie Hannaford for their constructive suggestions.

This work has been supported by the project MODEX-physically-based modelling of extreme hydrologic response under a probabilistic approach. Application to Dam Safety Analysis (CGL2011-22868), funded by the Spanish Ministry of Science and Innovation (now the Ministry of Economy and Competitiveness).

References

Acero, F.J., Gallego, M.C., García, J.A., 2012. Multi-day rainfall trends over the Iberian Peninsula. Theor. App. Climatol. 108(3-4):411-423.

Barredo, J.I., Saurí, D., Llasat, M.C., 2012. Assessing trends in insured losses from floods in Spain 1971-2008. Nat. Hazard Earth Sys. 12(5):1723-29.

Barriendos, M., Coeur, D., Lang, M., Llasat, M.C, Naulet, R., Lemaitre, F., Barrera, A., 2003. Stationarity analysis of historical flood series in France and Spain (14th-20th centuries). Nat. Hazard Earth Sys. 3:583-592.

Blöschl, G., Merz, R., Parajka, J., Salinas, J., Viglione, A., 2012. Floods in Austria. in: Kundzewicz Z.W. (Ed.), Changes in flood risk in Europe. CRC Press and IAHS Press, Wallingford, UK, pp. 169-177.

Brazdil, R., Kundzewicz, Z.W., Benito, G., Demaree, G., Macdonald, N., Roald, L. A., 2012. Historical floods in Europe in the past millennium, in: Kundzewicz Z.W. (Ed.), Changes in flood risk in Europe. CRC Press and IAHS Press, Wallingford, UK, pp. 121-166.

Burn, D.H., Sharif, M., Zhang, K., 2010. Detection of trends in hydrological extremes for Canadian watersheds. Hydrol. Process. 24: 1781–1790.

Castellarin, A., Pistocchi, A., 2012. An analysis of change in alpine annual maximum discharges: implications for the selection of design discharges. Hydrol. Process. 26(10):1517-26

Chebada, F., Ouarda, T.B.M.J., Duong, T.C., 2013. Testing for multivariate trends in hydrological frequency analysis. J. Hydrol. 486(0):519-30.

del Río, S., Herrero, L., Pinto-Gomes, C., Penas, A., 2011. Spatial analysis of mean temperature trends in Spain over the period 1961-2006. Global Planet. Change, 78: 65-75.

Giuntoli, I., Renard, B., Lang, M., 2012. Floods in France in: Kundzewicz Z.W. (Ed.), Changes in flood risk in Europe. CRC Press and IAHS Press, Wallingford, UK, pp. 199-211.

Hamed, K.H., 2009. Exact distribution of the Mann-Kendall trend test statistic for persistent data. J. Hydrol. 365: 86-94.

Hamed, K.H., Rao, A.R., 1998. A modified Mann-Kendall trend test for autocorrelated data. J. Hydrol. 204(1-4):182-96.

Hannaford, J., Buys, G., 2012. Trends in seasonal river flow regimes in the UK. J. Hydrol. 475(0):158-74.

Hannaford, J., Buys, G., Stahl, K., Tallaksen, L.M., 2013. The influence of decadal-scale variability on trends in long European streamflow records. Hydrol. Earth Syst. Sci., 17: 2717-2733.

Hargreaves, G.H., Allen, R.G., 2003. History and evaluation of Hargreaves evapotranspiration equation. J. Irrig. Drain Eng. 129: 53-63.

Heggen, R.J., 2001. Normalized antecedent precipitation index. J. Hydrol. Eng. 6(5): 377-381.

Herrera, S., Gutiérrez, J.M., Ancell, R., Pons, M.R., Frías, M.D., Fernández, J., 2012. Development and analysis of a 50-year high-resolution daily gridded precipitation dataset over Spain (Spain02). Int. J. Climatol. 32(1):74-85.

Hodgkins, G.A., Dudley, R.W., 2006. Changes in the timing of winter–spring streamflows in eastern North America, 1913–2002, Geophys. Res. Lett., 33: L06402.

Ishak, E.H., Rahman, A., Westra, S., Sharma, A., Kuczera, G., 2013. Evaluating the non-stationarity of Australian annual maximum flood. J. Hydrol. 494: 134-145.

Jiménez-Álvarez, A., García-Montañés, C., Mediero, L., Inicio, L., Garrote, J., 2012. Map of maximum flows of intercommunity basins, Revista de Obras Públicas, 3533, 7-32.

Khaliq M.N., Ouarda, T.B.M.J., Ondo J.C., Gachon, P., Bobée, B., 2006. Frequency analysis of a sequence of dependent and/or non-stationary hydro-meteorological observations: A review. J. Hydrol. 329(3):534-52.

Kohler, M.A., Linsley, R.K., 1951. Predicting runoff from storm rainfall. Res. Paper 34, U.S.Weather Bureau,Washington, D.C.

Kulkarni, A., von Storch, H., 1995. Monte Carlo experiments on the effect of serial correlation on the Mann-Kendall test of trend. Meteorol. Z. 4(2):82-85.

Kundzewicz, Z. W., Robson, A.J., 2004. Change detection in hydrological records- a review of the methodology. Hydrolog. Sci. J. 49(1): 7-19.

Kundzewicz, Z.W., Pińskwar, I., Brakenridge, G.R., 2013. Large floods in Europe, 1985–2009. Hydrolog. Sci. J. 58(1):1-7.

Kundzewicz, Z.W., Graczyk, D., Maurer, T., Pińskwar, I., Radziejewski, M., Svensson, C., Szwed, M., 2005. Trend detection in river flow series: 1. Annual maximum flow. Hydrolog. Sci. J. 50(5): 797-810.

Lang, M., Ouarda, T. B. M. J., Bobée, B., 1999. Towards operational guidelines for over-threshold modeling. J. Hydrol. 225: 103-117.

Libiseller, C., Grimvall, A., 2002. Performance of partial Mann–Kendall tests for trend detection in the presence of covariates. Environmetrics 13: 71–84.

Llasat, M.C., Barriendos, M., 2001. Availability and potential of historical flood series in the Iberian Peninsula (14th-20th centuries). In: The Use of Historical data in Natural Hazard Assessments (Glade, T., Albini, P. & Francés, F. Ed.). Kluwer Academic Publishers, Dordrecht, The Netherlands, pp.131-140.

Llasat, M.C., Rigo, T., Barriendos, M., 2003. The 'Montserrat-2000' flash-food event: a comparison with the floods that have occurred in the northeastern Iberian Peninsula since the 14th century. Int. J. Climatol. 23:453-469.

López-Moreno, J.I., Vicente-Serrano, S.M., Angulo-Martínez, M., Beguería, S., Kenawy, A., 2009. Trends in daily precipitation on the northeastern Iberian Peninsula, 1955-2006. Int. J. Climatol. 30(7):1026-41

López-Moreno, J.I., Beguería, S., García-Ruiz, J.M., 2006. Trends on high flows in the central Spanish Pyrenees: response to climatic factors or to land-use change? Hydrolog. Sci. J. 51(6):1039-50.

Lorenzo-Lacruz, J., Vicente-Serrano, S.M., López-Moreno, J.I., Morán-Tejeda, E., Zabalza, J., 2012. Recent trends in Iberian streamflows (1945-2005). J. Hydrol. 414–415(0):463-475.

Macdonald, N., Phillips, I.D., Mayle, G., 2010. Spatial and temporal variability of flood seasonality in Wales. Hydrol. Process. 24(13):1806-20.

Martínez-Fernández, J., Sánchez N., Herrero-Jiménez, C.M., 2013. Recent trends in rivers with near-natural flow regime: the case of the rivers headwaters in Spain. Prog. Phys. Geog. 37(4).

Merz, B., Vorogushyn, S., Uhlemann, S., Delgado, J., Hundecha, Y., 2012a. More efforts and scientific rigour are needed to attribute trends in flood time series. Hydrol. Earth Syst. Sci. 16, 1379-1387.

Merz, B., Kundzewicz, Z. W. , Delgado, J., Hundecha, Y., Kreibich, H., 2012b. Detection and attribution of changes in flood hazard and risk, in: Kundzewicz Z.W.

(Ed.), Changes in flood risk in Europe. CRC Press and IAHS Press, Wallingford, UK, pp. 435-458.

Milly, P.C.D., Betancourt, J., Falkenmark, M., Hirsch, R.M., Kundzewicz, Z.W., Lettenmaier, D.P., Stouffer, R.J., 2008. Stationarity is dead: Whither water management? Science, 318:573-74.

Morán-Tejeda, E., López-Moreno, J.I., Vicente-Serrano, S.M., Lorenzo-Lacruz, J., Ceballos-Barbancho, A., 2012. The contrasted evolution of high and low flows and precipitation indices in the Duero basin (Spain). Hydrol. Sci. J., 57(4): 591–611.

Morán-Tejeda, E., López-Moreno, J.I., Ceballos-Barbancho, A., Vicente-Serrano, S.M., 2011. River regimes and recent hydrological changes in the Duero basin (Spain). J. Hydrol. 404(3):241-58.

Moratiel, R., Durán, J.M., Snyder, R.L., 2010. Responses of reference evapotrsnpiration to changes in atmospheric humidity and air temperature in Spain. Clim. Res., 44: 27-40.

Murphy, C., Harrigan, S., Hall, J., Wilby, R. L., 2013. Climate-driven trends in mean and high flows from a network of reference stations in Ireland. Hydrolog. Sci. J, 58 (4), 755-772.

Onoz, B., Bayazit, M., 2012. Block bootstrapping for Mann-Kendall trend test of serially dependent data. Hydrol. Process. 26: 3552-3560.

Petrow, T., Merz, B., 2009. Trends in flood magnitude, frequency and seasonality in Germany in the period 1951-2002. J. Hydrol. 371(1):129-41

Pui, A., Lal, A., Sharma, A., 2011. How does the Interdecadal Pacific Oscillation affect design floods in Australia? Water Resour. Res., 47, W05554.

Rao, A., Hamed, K.H., 2000. Flood frequency analysis. CRC Press LLC, Boca Raton, FL, USA, pp. 1-10.

Sen, P.K., 1968. Estimates of the Regression Coefficient Based on Kendall's Tau. J. Am. Stat. Assoc. 63(324):1379-89.

Shuttleworth, W.J. 1993. Evaporation, in: Maidment, D.R. (Ed.), Handbook of hydrology. McGraw-Hill, New York, USA, pp. 4.1-4.53.

Sousa, P.M, Trigo, R.M., Aizpurua, P., Nieto, R., Gimeno, L., Garcia-Herrera, R., 2011. Trends and extremes of drought indices throughout the 20th century in the Mediterranean. Nat. Hazards Earth Syst. Sci., 11: 33–51.

Stahl, K., Tallaksen, L.M., Hannaford, J., van Lanen, H.A. J., 2012. Filling the white space on maps of European runoff trends: estimates from a multi-model ensemble. Hydrol. Earth Syst. Sci., 16: 2035-2047.

Stahl, K., Hisdal, H., Hannaford, J., Tallaksen, L. M., van Lanen, H. A. J., Sauquet, E., Demuth, S., Fendekova, M., Jódar, J., 2010. Streamflow trends in Europe: evidence from a dataset of near-natural catchments. Hydrol. Earth Syst. Sci. 14, 2367-2382.Svensson, C., Hannaford, J., Kundzewicz, Z.W., Marsh, T.J., 2006. Trends in floods: why is there no clear sign in observations?, in: Tchiguirinskaia, I., Thein, K.N.N., Hubert, P. (Eds.), Frontiers in Flood Research. IAHS Press, Wallingford, UK, pp 1-18.

Turco, M., Llasat, M.C., 2011. Trends in indices of daily precipitation extremes in Catalonia (NE, Spain), 1951-2003. Nat. Hazard Earth Sys. 11:3213-3226.

Valencia, J.L., Tarquis, A.M., Saá-Requejo, A., Gascó, J.M., 2012. Change of extreme rainfall indexes at Ebro River Basin. Nat. Hazard Earth Sys. 12:2127-2137.

von Storch, H., 1995. Misuses of statistical analysis in climate research, in: von Storch, H., Navarra, A. (Eds.), Analysis of climate variability: applications of statistical techniques. Springer-Verlag, Berlin, Germany, pp. 11–26.

Wilson, D., Hisdal, H., Lawrence, D., 2010. Has streamflow changed in the Nordic countries?- Recent trends and comparisons to hydrological projections. J. Hydrol. 394(3-4):334-46.

Yue, S., Wang, C.Y., 2002. Regional streamflow trend detection with consideration of both temporal and spatial correlation. Int. J. Climatol. 22 (8): 933-46.

Yue, S., Kundzewicz, Z.W., Wang, L., 2012. Detection of Changes, in: Kundzewicz Z.W. (Ed.), Changes in flood risk in Europe. CRC Press and IAHS Press, Wallingford, UK, pp. 387-408.

Yue, S., Pilon, P., Phinney, B., 2003. Canadian streamflow trend detection: impacts of serial and cross-correlation. Hydrolog. Sci. J. 48(1): 51-63.

Yue, S., Pilon, P. Cavadias, G., 2002. Power of the Mann-Kendall and Sperman's rho test for detecting monotonic trends in hydrological series. J. Hydrol. 259(1-4):254-71.

Figure 1. Spatial distribution of Spanish river basin authorities. Selected gauging sites used in the study are represented by solid black points.

Figure 2. Trends in AMF series for the periods: a) 1942-2009, b) 1949-2009 and c) 1959-2009. Trends in AMFD series for the periods: d) 1942-2009, e) 1949-2009 and f) 1959-2009. Significant trends are plotted by triangles. Magnitude of triangles depend on the magnitude of trend (β), which is standardised for the case of AMF. Non-significant trends are plotted by black points.

Figure 3. Trends in seasonal floods. Seasons are presented by rows and periods by columns. Significant trends are plotted by triangles. Magnitude of triangles depend on the standardised magnitude of trend (β). Non-significant trends are plotted by black points.

Figure 4. Trends in POT3 series variables: magnitude in the first row, annual frequency in the second row and mean day of flood in the third row. Periods are presented by columns. Significant trends are plotted by triangles. Magnitude of triangles depend on the magnitude of trend (β), which is standardised for the case of POT3M. Non-significant trends are plotted by black points.

Figure 5. Slope of significant trends for a varying length moving window for the ten longest AMF series. Non-significant trends are plotted by green cells. Slopes are standardised by the mean of each AMF series.

Figure 6. AMF series for gauging stations D2, T2 and E18. Dashed lines show the mean value for each site.

Figure 7. Slope of significant trends for a varying length moving window for the ten longest POT3 series. Non-significant trends are plotted by green cells. Slopes are standardised by the mean of each POT3 series.

Figure 8. Annual occurrences in POT3 series for gauging stations D2, T2 and E18. Dashed lines show the mean value for each site.

Figure 9. Significant trends in annual maximum cumulative precipitation on one, *AMP1*, three, *AMP3*, and five, *AMP5*, consecutive days, and annual cumulative precipitation, *AP*, series. Non-significant trends are plotted by white cells. Solid black triangles and circles show significant and non-significant trends, respectively, in AMF series after removing the effect of the corresponding variable through the PMK test.

Figure 10. Significant trends in the antecedent precipitation index, *API*, the ratio of annual runoff to precipitation, *AR/AP*, and annual evapotranspiration, *ET*, series. Non-significant trends are plotted by white cells. Solid black triangles and circles show significant and non-significant trends, respectively, in AMF series after removing the effect of the corresponding variable through the PMK test.

Figure 1

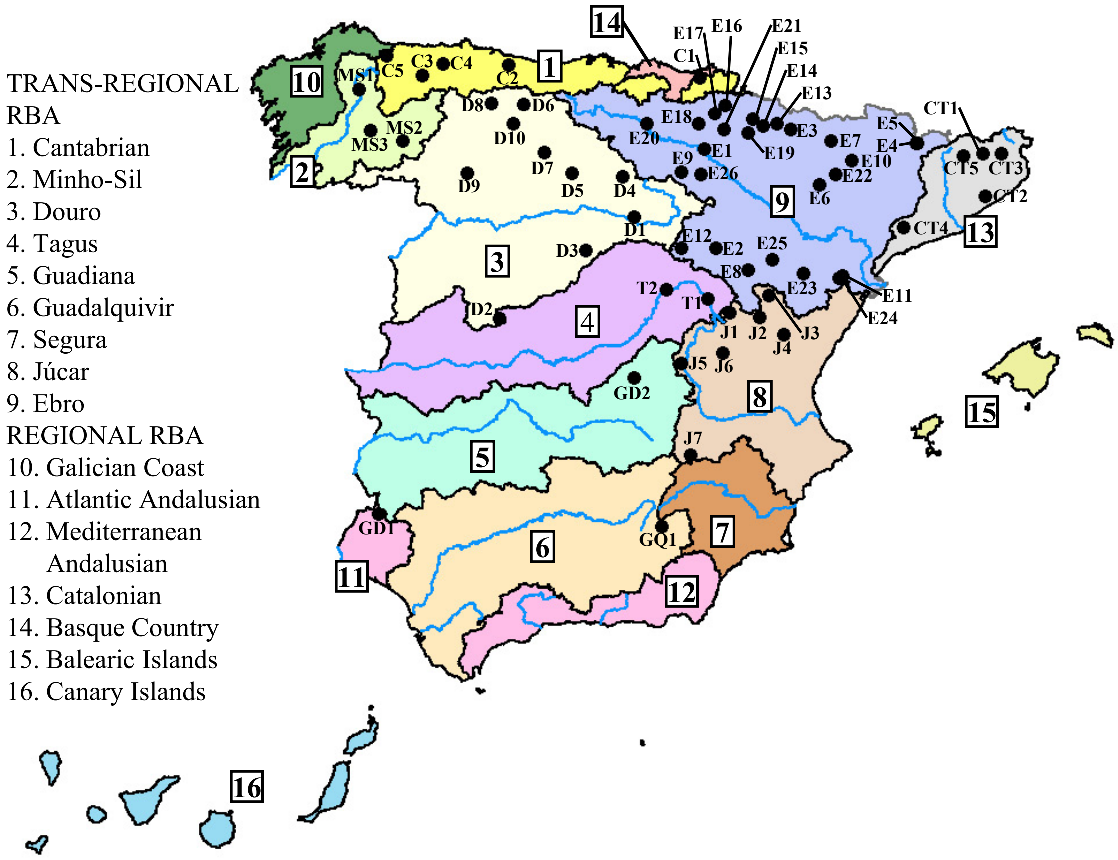

TRANS-REGIONAL RBA
1. Cantabrian
2. Minho-Sil
3. Douro
4. Tagus
5. Guadiana
6. Guadalquivir
7. Segura
8. Júcar
9. Ebro
REGIONAL RBA
10. Galician Coast
11. Atlantic Andalusian
12. Mediterranean Andalusian
13. Catalonian
14. Basque Country
15. Balearic Islands
16. Canary Islands
1
2
3
4
5
6
7
8
9
10
11
12
13
14
15
16
MS1
MS2
MS3
C1
C2
C3
C4
C5
D1
D2
D3
D4
D5
D6
D7
D8
D9
D10
E1
E2
E3
E4
E5
E6
E7
E8
E9
E10
E11
E12
E13
E14
E15
E16
E17
E18
E19
E20
E21
E22
E23
E24
E25
E26
CT1
CT2
CT3
CT4
CT5
T1
T2
J1
J2
J3
J4
J5
J6
J7
GD1
GD2
GQ1

Figure 2

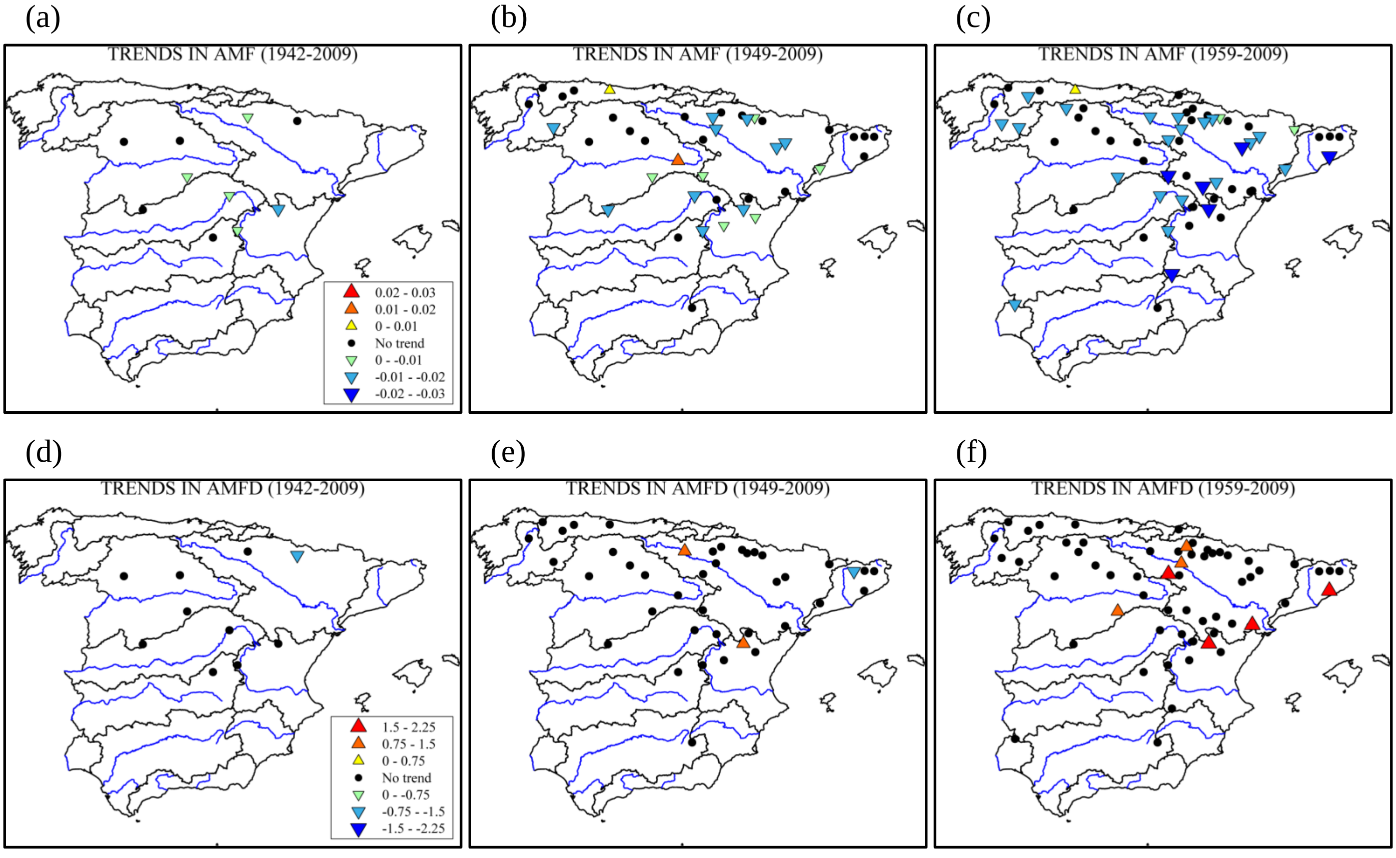
(a)
TRENDS IN AMF (1942-2009)
0.02 - 0.03
0.01 - 0.02
0 - 0.01
No trend
0 - -0.01
-0.01 - -0.02
-0.02 - -0.03
(b)
TRENDS IN AMF (1949-2009)
(c)
TRENDS IN AMF (1959-2009)
(d)
TRENDS IN AMFD (1942-2009)
1.5 - 2.25
0.75 - 1.5
0 - 0.75
No trend
0 - -0.75
-0.75 - -1.5
-1.5 - -2.25
(e)
TRENDS IN AMFD (1949-2009)
(f)
TRENDS IN AMFD (1959-2009)

Figure 3

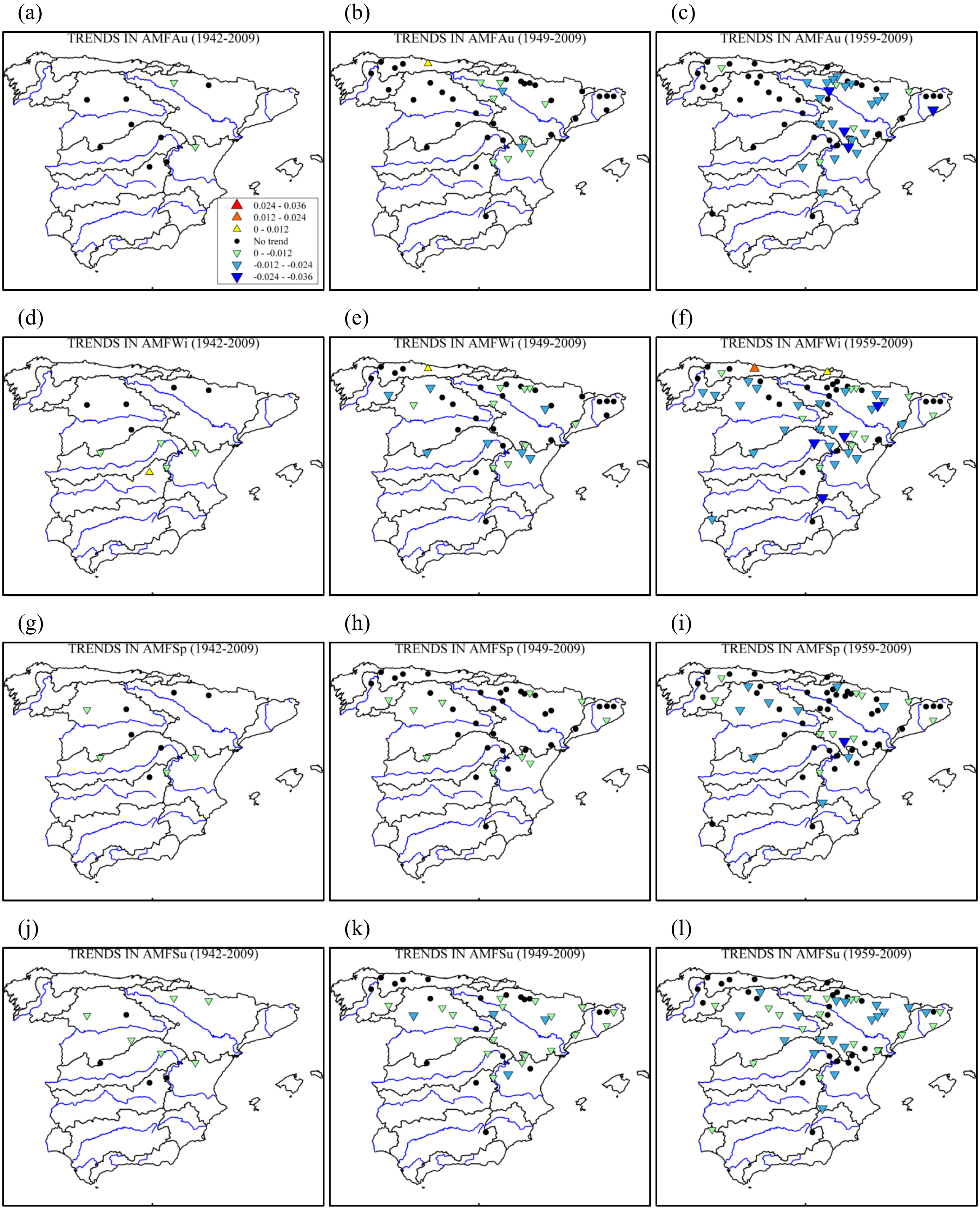
(a)
TRENDS IN AMFAu (1942-2009)
0.024 - 0.036
0.012 - 0.024
0 - 0.012
No trend
0 - -0.012
-0.012 - -0.024
-0.024 - -0.036
(b)
TRENDS IN AMFAu (1949-2009)
(c)
TRENDS IN AMFAu (1959-2009)
(d)
TRENDS IN AMFWi (1942-2009)
(e)
TRENDS IN AMFWi (1949-2009)
(f)
TRENDS IN AMFWi (1959-2009)
(g)
TRENDS IN AMFSp (1942-2009)
(h)
TRENDS IN AMFSp (1949-2009)
(i)
TRENDS IN AMFSp (1959-2009)
(j)
TRENDS IN AMFSu (1942-2009)
(k)
TRENDS IN AMFSu (1949-2009)
(l)
TRENDS IN AMFSu (1959-2009)

Figure 4

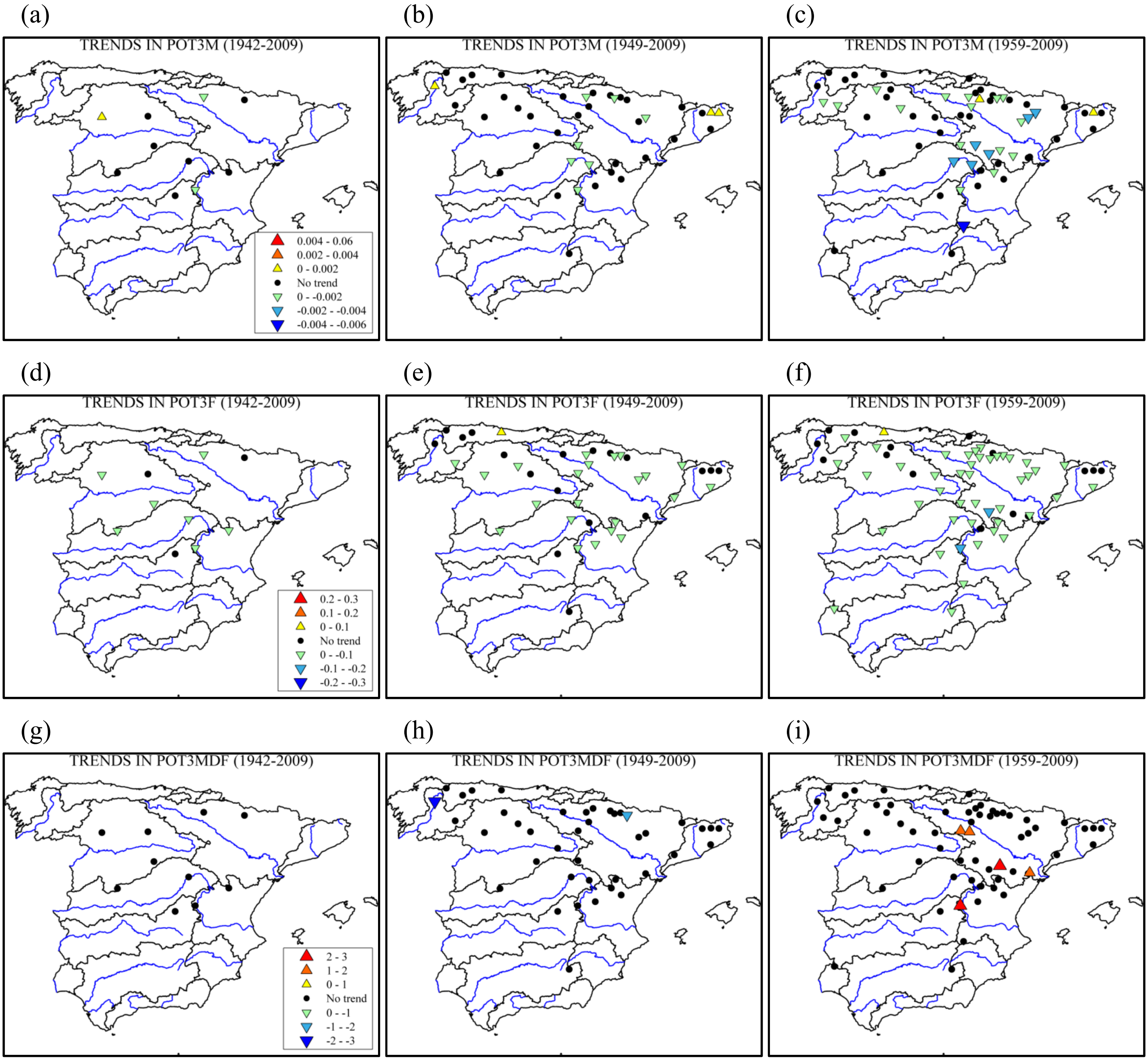
(a)
TRENDS IN POT3M (1942-2009)
0.004 - 0.06
0.002 - 0.004
0 - 0.002
No trend
0 - -0.002
-0.002 - -0.004
-0.004 - -0.006
(b)
TRENDS IN POT3M (1949-2009)
(c)
TRENDS IN POT3M (1959-2009)
(d)
TRENDS IN POT3F (1942-2009)
0.2 - 0.3
0.1 - 0.2
0 - 0.1
No trend
0 - -0.1
-0.1 - -0.2
-0.2 - -0.3
(e)
TRENDS IN POT3F (1949-2009)
(f)
TRENDS IN POT3F (1959-2009)
(g)
TRENDS IN POT3MDF (1942-2009)
2 - 3
1 - 2
0 - 1
No trend
0 - -1
-1 - -2
-2 - -3
(h)
TRENDS IN POT3MDF (1949-2009)
(i)
TRENDS IN POT3MDF (1959-2009)

Figure 5

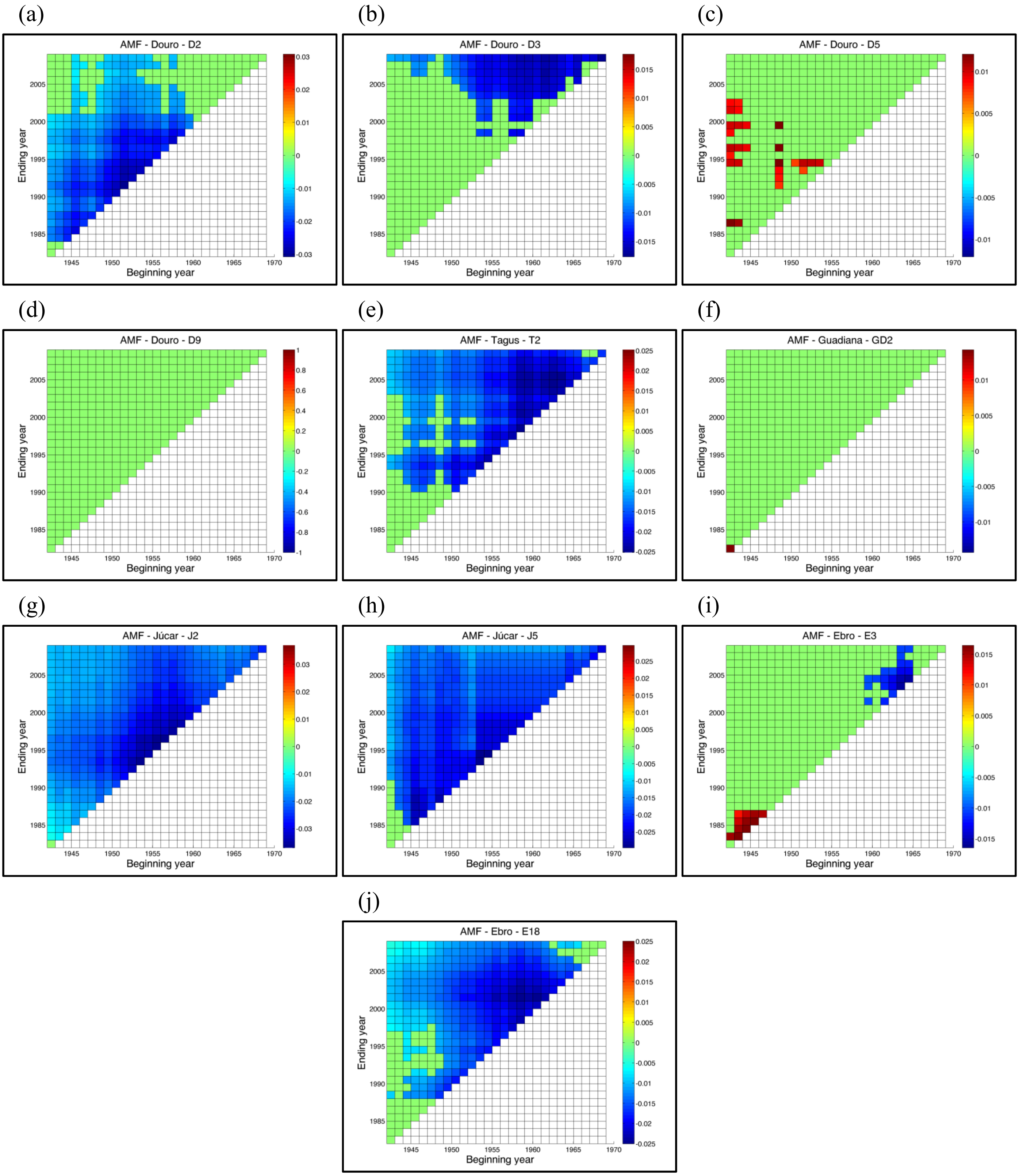
(a)
AMF - Douro - D2
(b)
AMF - Douro - D3
(c)
AMF - Douro - D5
(d)
AMF - Douro - D9
(e)
AMF - Tagus - T2
(f)
AMF - Guadiana - GD2
(g)
AMF - Júcar - J2
(h)
AMF - Júcar - J5
(i)
AMF - Ebro - E3
(j)
AMF - Ebro - E18
Ending year
Beginning year
1945
1950
1955
1960
1965
1970
1985
1990
1995
2000
2005

Figure 6

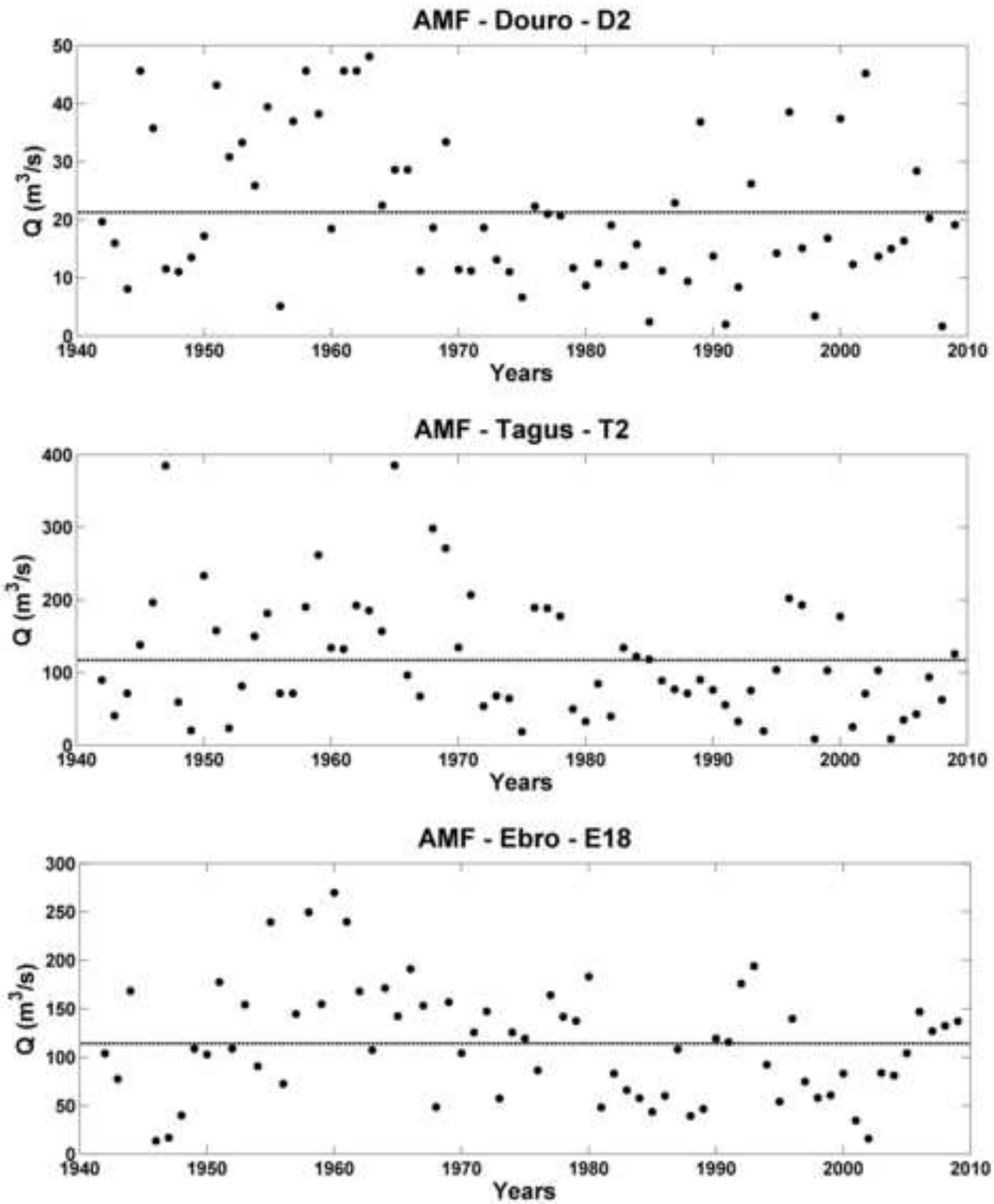
AMF - Douro - D2
Q (m3/s)
50
40
30
20
10
0
1940
1950
1960
1970
1980
1990
2000
2010
Years
AMF - Tagus - T2
Q (m3/s)
400
300
200
100
0
1940
1950
1960
1970
1980
1990
2000
2010
Years
AMF - Ebro - E18
Q (m3/s)
300
250
200
150
100
50
0
1940
1950
1960
1970
1980
1990
2000
2010
Years

Figure 7

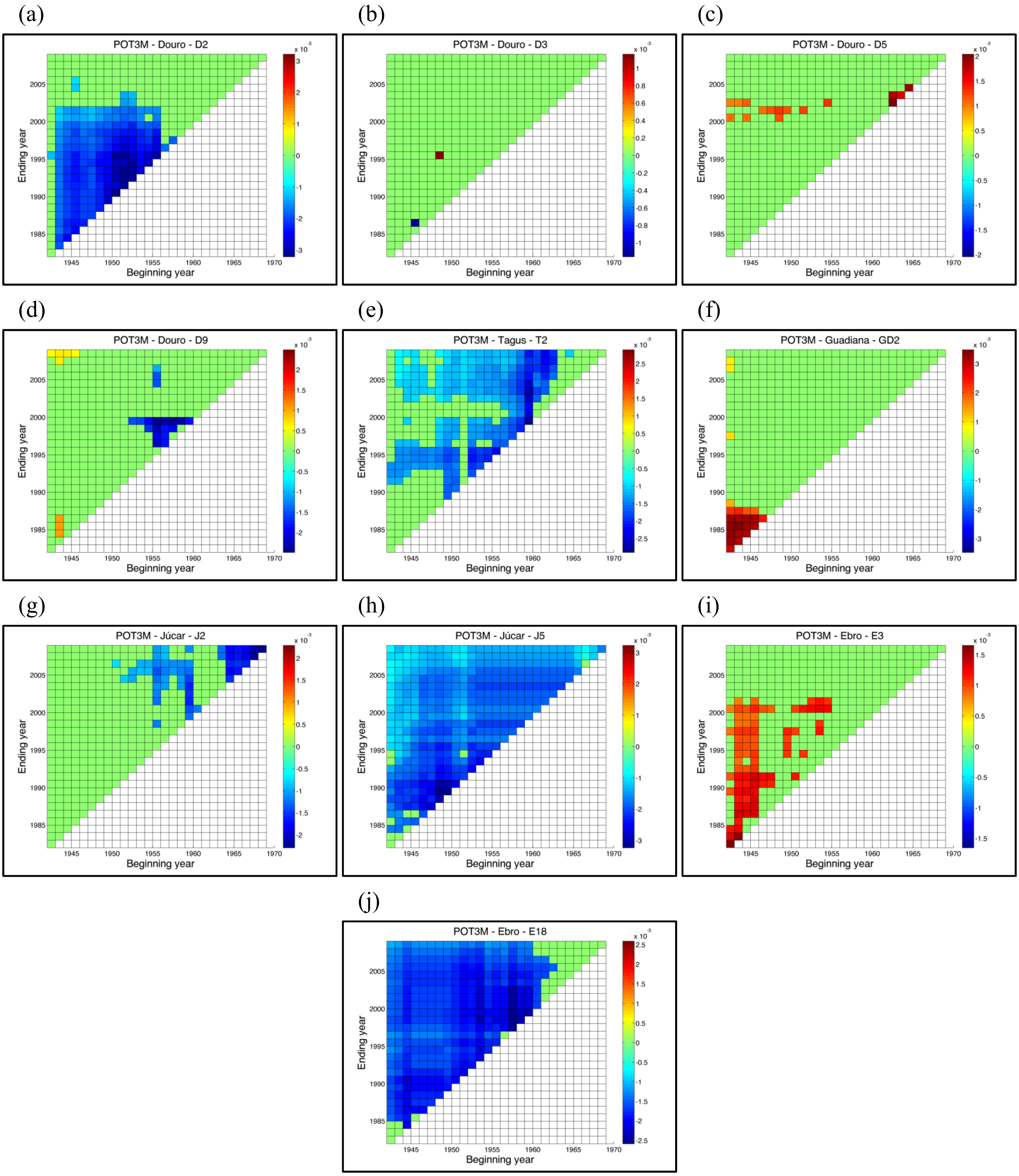
(a)
POT3M - Douro - D2
(b)
POT3M - Douro - D3
(c)
POT3M - Douro - D5
(d)
POT3M - Douro - D9
(e)
POT3M - Tagus - T2
(f)
POT3M - Guadiana - GD2
(g)
POT3M - Júcar - J2
(h)
POT3M - Júcar - J5
(i)
POT3M - Ebro - E3
(j)
POT3M - Ebro - E18
Ending year
Beginning year
1945
1950
1955
1960
1965
1970
1985
1990
1995
2000
2005
x 10^-3

Figure 8

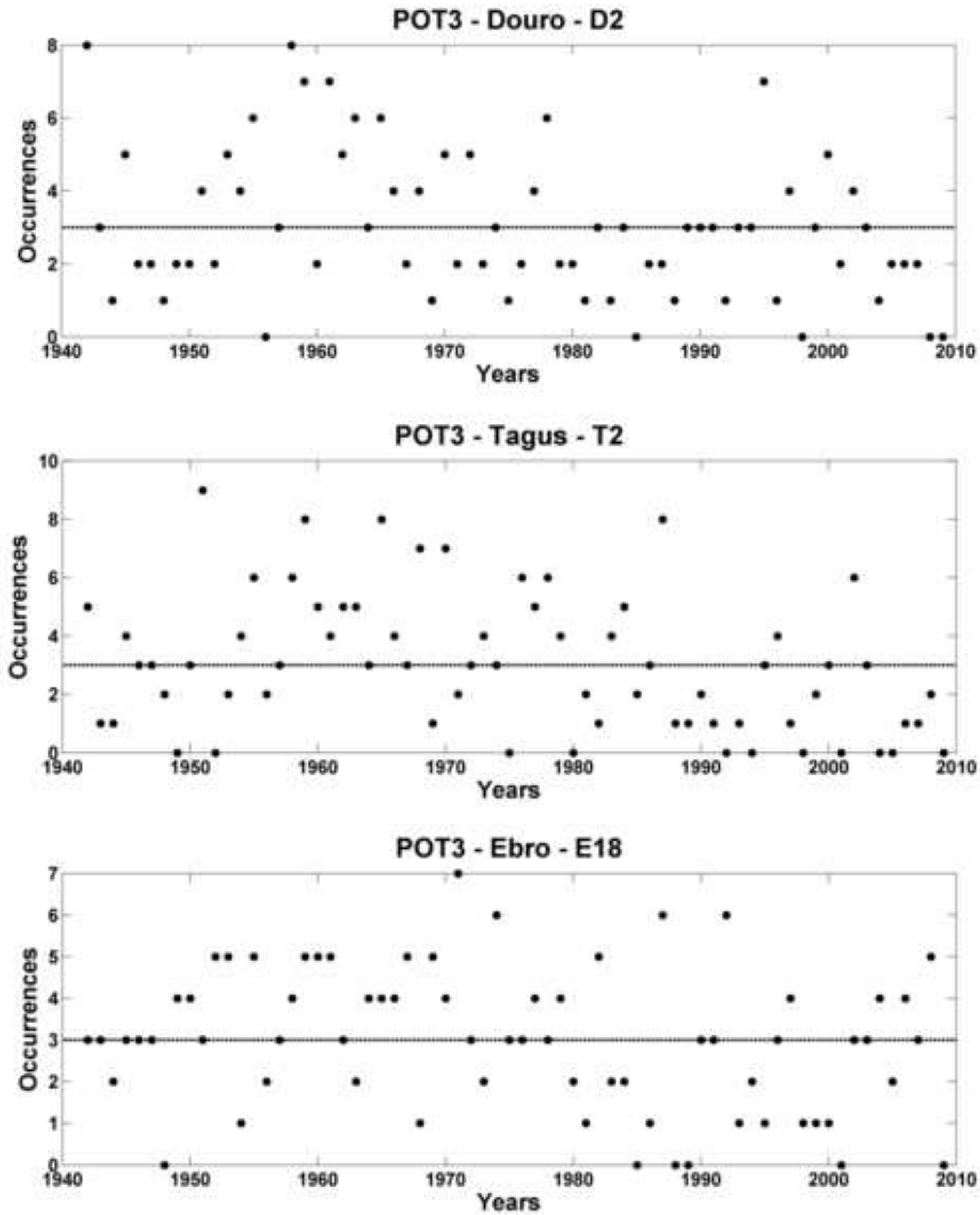
POT3 - Douro - D2
Occurrences
Years
POT3 - Tagus - T2
Occurrences
Years
POT3 - Ebro - E18
Occurrences
Years

Figure 9

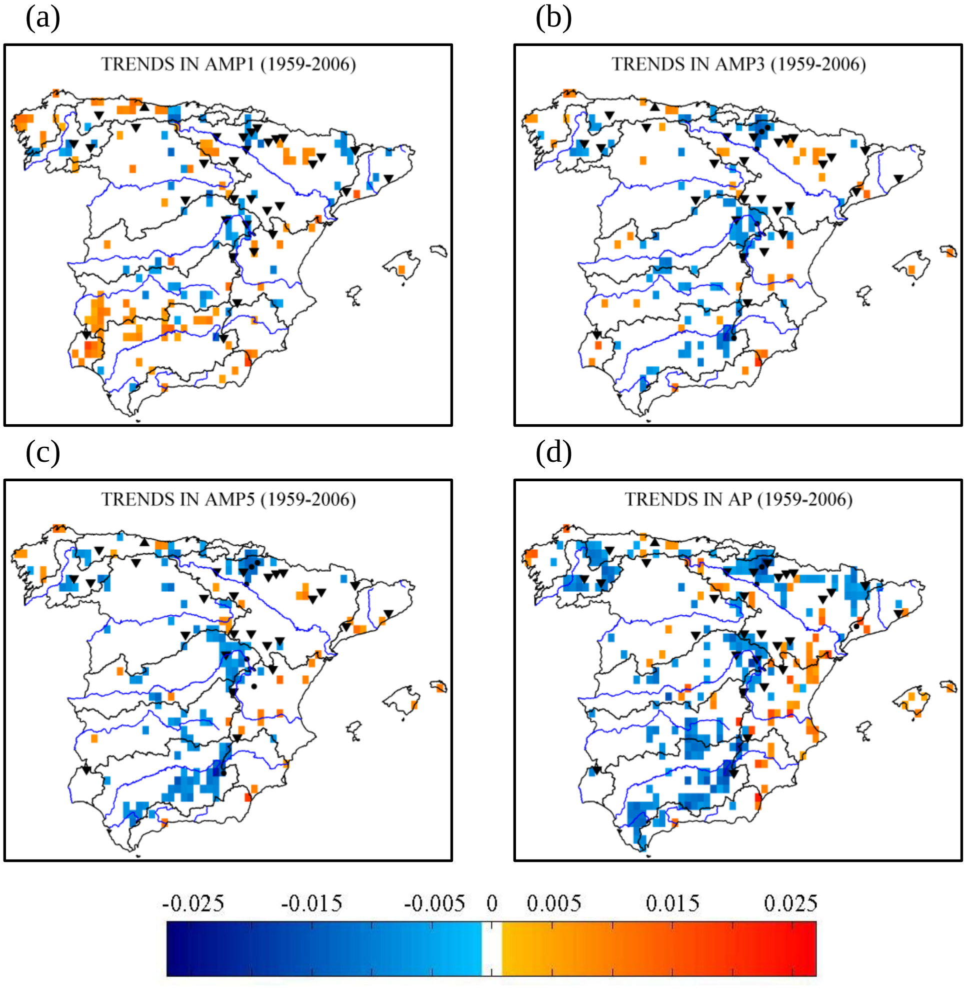
(a)
TRENDS IN AMP1 (1959-2006)
(b)
TRENDS IN AMP3 (1959-2006)
(c)
TRENDS IN AMP5 (1959-2006)
(d)
TRENDS IN AP (1959-2006)
-0.025
-0.015
-0.005
0
0.005
0.015
0.025

Figure 10

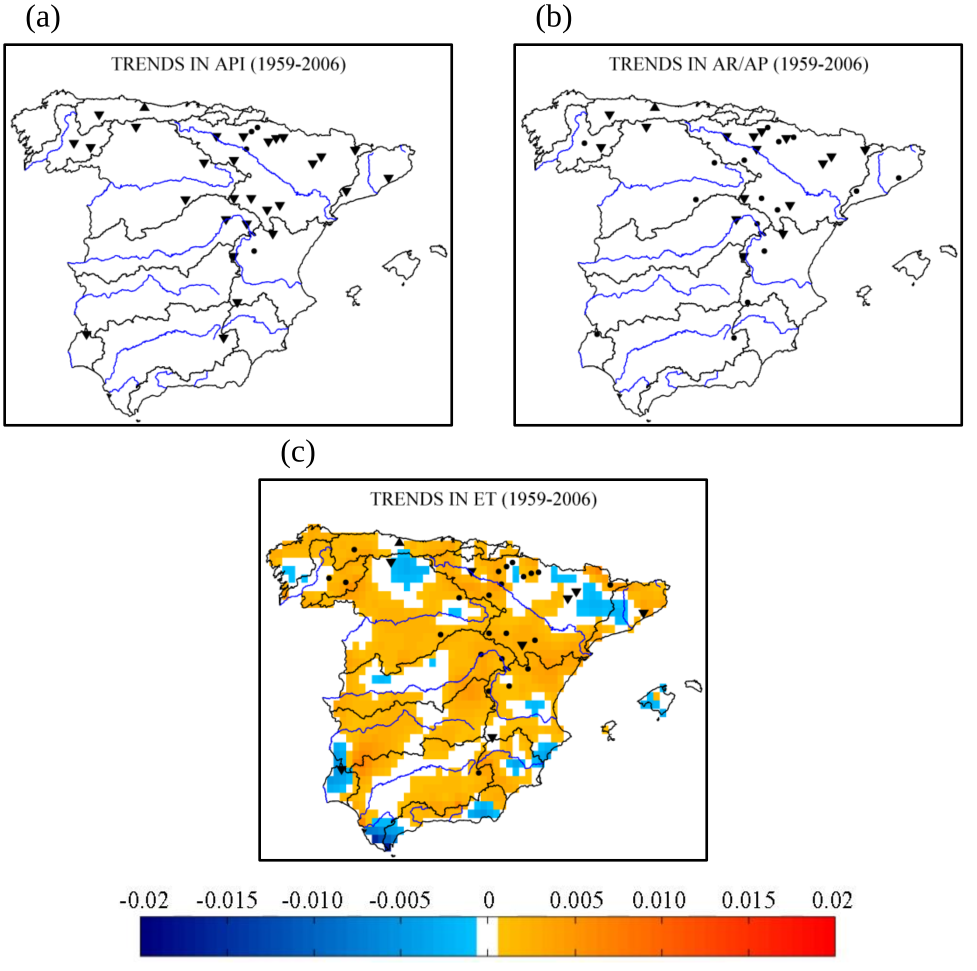
(a)
TRENDS IN API (1959-2006)
(b)
TRENDS IN AR/AP (1959-2006)
(c)
TRENDS IN ET (1959-2006)
-0.02
-0.015
-0.010
-0.005
0
0.005
0.010
0.015
0.02

Hydro-climatic variable	Abbreviation	Description
Annual maximum flow (m^3/s)	AMF	Maximum mean daily flow in a hydrological year (October-September)
Day of AMF (days)	AMFD	Day of occurrence of AMF
Annual maximum flow in autumn (m^3/s)	AMFAu	Maximum mean daily flow in autumn (October-December)
Annual maximum flow in winter (m^3/s)	AMFWi	Maximum mean daily flow in winter (January-March)
Annual maximum flow in spring (m^3/s)	AMFSp	Maximum mean daily flow in spring (April-June)
Annual maximum flow in summer (m^3/s)	AMFSu	Maximum mean daily flow in summer (July-September)
Peaks-over-threshold magnitude (m^3/s)	POT3M	Flow peaks over the threshold that leads to an average of three events per year
Peaks-over-threshold frequency (events per year)	POT3F	Annual number of flow peaks in POT3 series
Mean day of flood occurrence (days)	MDF	Mean day of occurrence of the POT3 series for each hydrological year
Annual maximum cumulative precipitation in X days (mm)	AMPX	Annual maximum cumulative precipitation in consecutive X days for each hydrological year (October-September)
Annual precipitation (mm)	AP	Cumulative annual precipitation in hydrological years
Annual evapotranspiration (mm)	ET	Cumulative annual evapotranspiration in hydrological years
Antecedent precipitation index (mm)	API	Antecedent precipitation index the day before the occurrence of AMF
Annual runoff to precipitation (-)	AR/AP	Ratio of cumulative annual runoff in mm to AP

Table 1: Hydro-climatic variables used in the study

RBA	Code	Area (km^2)	RBA	Code	Area (km^2)
Cantabrian (C)	C1	775	Ebro (E)	E1	1445
	C2	486		E2	732
	C3	531		E3	238
	C4	403		E4	559
	C5	712		E5	1233
Minho-Sil (MS)	MS1	2303		E6	765
	MS2	558		E7	626
	MS3	337		E8	1498
Douro (D)	D1	900		E9	223
	D2	88		E10	426
	D3	280		E11	48
	D4	349		E12	196
	D5	2413		E13	161
	D6	32		E14	506
	D7	312		E15	396
	D8	154		E16	240
	D9	650		E17	1756
	D10	355		E18	943
Tagus (T)	T1	410		E19	275
	T2	3253		E20	307
Guadiana (GD)	GD1	88		E21	47
	GD2	995		E22	345
Guadalquivir (GQ)	GQ1	28		E23	141
				E24	49
Júcar (J)	J1	95		E25	138
	J2	1396		E26	326
	J3	478	Catalonian (CT)	CT1	128
	J4	665		CT2	125
	J5	187		CT3	804
	J6	829		CT4	338
	J7	75		CT5	738

Table 2. Selected gauging sites used in the study divided into groups according to River Basin Authorities (RBAs).

	All stations	
	Down	Up
AMF	**5 (50)**	0 (0)
AMFD	**1 (10)**	0 (0)
AMFAu	**2 (20)**	0 (0)
AMFWi	**4 (40)**	1 (10)
AMFSp	**4 (40)**	0 (0)
AMFSu	**6 (60)**	0 (0)
POT3M	2 (20)	1 (10)
POT3F	**7 (70)**	0 (0)
POT3MDF	0 (0)	0 (0)

Table 3. Number and percentage (in brackets) of gauging stations showing significant trends for the period 1942-2009. Field significant trends are highlighted in bold.

	All stations		Douro		Ebro		Júcar	
	Down	Up	Down	Up	Down	Up	Down	Up
AMF	**16 (38)**	2 (5)	**2 (29)**	**1 (14)**	**7 (47)**	0 (0)	**4 (80)**	0 (0)
AMFD	1 (2)	2 (5)	0 (0)	0 (0)	0 (0)	1 (7)	0 (0)	**1 (20)**
AMFAu	**10 (24)**	1 (3)	0 (0)	0 (0)	**5 (33)**	0 (0)	**5 (100)**	0 (0)
AMFWi	**16 (38)**	1 (2)	**3 (43)**	0 (0)	**5 (33)**	0 (0)	**5 (100)**	0 (0)
AMFSp	**10 (24)**	0 (0)	**3 (43)**	0 (0)	**2 (13)**	0 (0)	**3 (60)**	0 (0)
AMFSu	**23 (55)**	0 (0)	**4 (57)**	0 (0)	**10 (67)**	0 (0)	**4 (80)**	0 (0)
POT3M	7 (17)	3 (7)	0 (0)	0 (0)	**4 (27)**	0 (0)	**1 (20)**	0 (0)
POT3F	**23 (55)**	1 (2)	**4 (57)**	0 (0)	**10 (67)**	0 (0)	**5 (100)**	0 (0)
POT3MDF	0 (0)	0 (0)	0 (0)	0 (0)	1 (7)	0 (0)	0 (0)	0 (0)

Table 4. Number and percentage (in brackets) of gauging stations that show significant trends for the period 1949-2009. Field significant trends are highlighted in bold.

	All stations		Douro		Ebro		Júcar	
	Down	Up	Down	Up	Down	Up	Down	Up
AMF	**27 (44)**	1 (2)	**2 (20)**	0 (0)	**14 (54)**	0 (0)	**3 (43)**	0 (0)
AMFD	0 (0)	**7 (11)**	0 (0)	1 (10)	0 (0)	**4 (15)**	0 (0)	**1 (14)**
AMFAu	**27 (44)**	0 (0)	0 (0)	0 (0)	**18 (69)**	0 (0)	**6 (86)**	0 (0)
AMFWi	**36 (59)**	2 (3)	**7 (70)**	0 (0)	**15 (58)**	0 (0)	**6 (86)**	0 (0)
AMFSp	**20 (33)**	0 (0)	**5 (50)**	0 (0)	**9 (35)**	0 (0)	**3 (43)**	0 (0)
AMFSu	**38 (62)**	0 (0)	**8 (80)**	0 (0)	**20 (77)**	0 (0)	**3 (43)**	0 (0)
POT3M	**22 (36)**	2 (3)	2 (20)	0 (0)	**13 (50)**	1 (4)	**3 (43)**	0 (0)
POT3F	**45 (74)**	1 (2)	**7 (70)**	0 (0)	**23 (88)**	0 (0)	**6 (86)**	0 (0)
POT3MDF	0 (0)	5 (8)	0 (0)	0 (0)	0 (0)	**4 (15)**	0 (0)	**1 (14)**

Table 5. Number and percentage (in brackets) of gauging stations that show significant trends for the period 1959-2009. Field significant trends are highlighted in bold.

RBA	Code	AMF	AMP1	AMP3	AMP5	AP	ET	API	AR/AP
Cantabrian	C2	↑			-	-	-	↑	-
	C3	↓	-	-	-	-	↑	-	-
Minho-Sil	MS2	↓		-	↓	↓	↑	-	-
	MS3	↓	-	-	-	-	↑	-	-
Douro	D3	↓	-	-	-	-	↑	-	↓
	D4	↓	-	-	-	-	↑	-	↓
	D8	↓	-	-	-	-	-	-	-
Tagus	T1	↓			-	-	↑	-	-
	T2	↓		↓	↓	↓	↑	-	-
Guadiana	GD1	↓	-	-	-	-	-	-	-
Guadalquivir	GQ1	↓	-	-	-	-	↑	-	-
Júcar	J2	↓	-	-	-	-	↑	-	↓
	J5	↓	-	↓	↓	-	↑	-	↓
	J6	↓		-	-	-	↑	-	↓
	J7	↓	-	-	-	-	-	-	↓
Ebro	E1	↓			↓	↓	↑	↓	-
	E2	↓		-	-	-	↑	-	↓
	E4	↓	-	-	-	-	↑	-	↓
	E5	↓	-	-	-	-	↑	-	↓
	E8	↓	-	-	-	-	↑	-	↓
	E9	↓	-	-	-	-	↑	-	↓
	E10	↓	-	-	-	-	-	-	↓
	E12	↓	-	-	-	-	↑	-	↓
	E13	↓	-	-	-	-	↑	-	↓
	E14	↓	-	-	-	-	↑	↑	↓
	E16	↓	-			↓	↑	-	↓
	E17	↓	-	↓	↓	↓	↑	↓	-
	E18	↓				↓	↑	↓	↓
	E19	↓	↑	-	-	-	↑	-	↓
	E20	↓	-	-	-	-	↑	-	-
	E22	↓	↑	↑	-	-	-	-	↓
	E25	↓	-	-	-	-	↑	-	↓
Catalonian	CT2	↓	-	-	-	-	↑	-	↓
	CT4	↓	-		-	-	↑	-	↓

Table 6. Summary of trends in climatic variables in gauging stations where flood trends in AMF series were detected for the period 1959-2006. Signs of significant trends are represented by arrows. Dashes represent no trends.

RBA	Code	AMF	Conditioned PMK							Driver
			AMP1	AMP3	AMP5	AP	ET	API	AR/AP	
Cantabrian	C2	↑	↑	↑	↑	↑	↑	↑	↑	ND
	C3	↓	↓	↓	↓	↓	-	↓	↓	ET
Minho-Sil	MS2	↓	↓	↓	↓	↓	-	↓	↓	ET
	MS3	↓	↓	↓	↓	↓	-	↓	-	ET-AR/AP
Douro	D3	↓	↓	↓	↓	↓	-	↓	-	ET-AR/AP
	D4	↓	↓	↓	↓	↓	-	↓	-	ET-AR/AP
	D8	↓	↓	↓	↓	↓	↓	↓	↓	ND
Tagus	T1	↓	↓	-	-	↓	-	↓	-	AMP-ET-AR/AP
	T2	↓	↓	↓	↓	↓	-	↓	↓	ET
Guadiana	GD1	↓	↓	↓	↓	↓	↓	↓	-	AR/AP
Guadalquivir	GQ1	↓	↓	-	-	↓	-	↓	-	AMP-ET-AR/AP
Júcar	J2	↓	↓	↓	↓	↓	-	↓	↓	ET
	J5	↓	↓	↓	↓	↓	-	↓	↓	ET
	J6	↓	↓	↓	-	↓	-	-	-	AMP-ET-AP-AR/AP
	J7	↓	↓	↓	↓	↓	↓	↓	-	AR/AP
Ebro	E1	↓	↓	-	-	-	-	-	↓	AMP-AP-ET-API
	E2	↓	↓	↓	↓	↓	-	↓	-	ET-AR/AP
	E4	↓	↓	↓	↓	↓	-	↓	↓	ET
	E5	↓	↓	↓	↓	↓	-	↓	-	ET-AR/AP
	E8	↓	↓	↓	↓	↓	↓	↓	-	AR/AP
	E9	↓	↓	↓	↓	↓	-	↓	-	ET-AR/AP
	E10	↓	↓	↓	↓	↓	↓	↓	↓	ND
	E12	↓	↓	↓	↓	↓	-	↓	↓	ET
	E13	↓	↓	↓	↓	↓	-	↓	-	ET-AR/AP
	E14	↓	↓	↓	↓	↓	-	↓	↓	ET
	E16	↓	↓	-	-	↓	-	-	-	AMP-ET-API-AR/AP
	E17	↓	↓	-	-	-	-	-	↓	AMP-AP-ET-API
	E18	↓	↓	↓	↓	↓	-	↓	↓	ET
	E19	↓	↓	↓	↓	↓	-	↓	-	ET-AR/AP
	E20	↓	↓	↓	↓	↓	-	↓	↓	ET
	E22	↓	↓	↓	↓	↓	↓	↓	↓	ND
	E25	↓	↓	↓	↓	↓	↓	↓	↓	ND
Catalonian	CT2	↓	↓	↓	↓	↓	-	↓	-	ET-AR/AP
	CT4	↓	↓	↓	↓	-	↓	↓	-	AP-AR/AP

Table 7. Summary of links to climatic variables in gauging stations where flood trends in AMF series were detected for the period 1959-2006. Signs of significant trends are represented by arrows. Dashes represent no trends. ND = No driver.

Highlights:

A representative set of gauging sites with negligible dam regulation was obtained

Both magnitude and frequency of floods tend to decrease in Spain

Decreasing trends could be conditioned on a flood-rich period in 1950-1970

Flood trends were linked to increasing evapotranspiration in last decades